NASA/TM—2012-217728

Integrated Structural/Acoustic Modeling of Heterogeneous Panels

Brett A. Bednarcyk
Glenn Research Center, Cleveland, Ohio

Jacob Aboudi
Tel-Aviv University, Ramat-Aviv, Israel

Steven M. Arnold and James A. Pennline
Glenn Research Center, Cleveland, Ohio

October 2012

NASA STI Program . . . in Profile

Since its founding, NASA has been dedicated to the advancement of aeronautics and space science. The NASA Scientific and Technical Information (STI) program plays a key part in helping NASA maintain this important role.

The NASA STI Program operates under the auspices of the Agency Chief Information Officer. It collects, organizes, provides for archiving, and disseminates NASA's STI. The NASA STI program provides access to the NASA Aeronautics and Space Database and its public interface, the NASA Technical Reports Server, thus providing one of the largest collections of aeronautical and space science STI in the world. Results are published in both non-NASA channels and by NASA in the NASA STI Report Series, which includes the following report types:

- TECHNICAL PUBLICATION. Reports of completed research or a major significant phase of research that present the results of NASA programs and include extensive data or theoretical analysis. Includes compilations of significant scientific and technical data and information deemed to be of continuing reference value. NASA counterpart of peer-reviewed formal professional papers but has less stringent limitations on manuscript length and extent of graphic presentations.

- TECHNICAL MEMORANDUM. Scientific and technical findings that are preliminary or of specialized interest, e.g., quick release reports, working papers, and bibliographies that contain minimal annotation. Does not contain extensive analysis.

- CONTRACTOR REPORT. Scientific and technical findings by NASA-sponsored contractors and grantees.

- CONFERENCE PUBLICATION. Collected papers from scientific and technical conferences, symposia, seminars, or other meetings sponsored or cosponsored by NASA.

- SPECIAL PUBLICATION. Scientific, technical, or historical information from NASA programs, projects, and missions, often concerned with subjects having substantial public interest.

- TECHNICAL TRANSLATION. English-language translations of foreign scientific and technical material pertinent to NASA's mission.

Specialized services also include creating custom thesauri, building customized databases, organizing and publishing research results.

For more information about the NASA STI program, see the following:

- Access the NASA STI program home page at *http://www.sti.nasa.gov*

- E-mail your question to *help@sti.nasa.gov*

- Fax your question to the NASA STI Information Desk at 443–757–5803

- Phone the NASA STI Information Desk at 443–757–5802

- Write to:
  STI Information Desk
  NASA Center for AeroSpace Information
  7115 Standard Drive
  Hanover, MD 21076–1320

NASA/TM—2012-217728

Integrated Structural/Acoustic Modeling of Heterogeneous Panels

Brett A. Bednarcyk
Glenn Research Center, Cleveland, Ohio

Jacob Aboudi
Tel-Aviv University, Ramat-Aviv, Israel

Steven M. Arnold and James A. Pennline
Glenn Research Center, Cleveland, Ohio

National Aeronautics and
Space Administration

Glenn Research Center
Cleveland, Ohio 44135

October 2012

This work was sponsored by the Fundamental Aeronautics Program
at the NASA Glenn Research Center.

Level of Review: This material has been technically reviewed by technical management.

Available from

NASA Center for Aerospace Information
7115 Standard Drive
Hanover, MD 21076–1320

National Technical Information Service
5301 Shawnee Road
Alexandria, VA 22312

Available electronically at http://www.sti.nasa.gov

Integrated Structural/Acoustic Modeling of Heterogeneous Panels

Brett A. Bednarcyk
National Aeronautics and Space Administration
Glenn Research Center
Cleveland, Ohio 44135

Jacob Aboudi
Tel-Aviv University
Ramat-Aviv 69978, Israel

Steven M. Arnold and James A. Pennline
National Aeronautics and Space Administration
Glenn Research Center
Cleveland, Ohio 44135

Introduction

A continuum model is developed for the analysis and prediction of the dynamic response of multiphase panels that are subjected to impulsive loading. The multiphase medium consists of any number of different elastic anisotropic constituents including the case of voids. The impulsive loading is applied on the external boundaries of panel in the form of time-dependent tractions and/or displacements. Acoustic loading can thus be modeled as a time-dependent pressure wave. The derived continuum theory results in a system of second-order equations in time. This system represents the governing elastodynamic equations for the discretized regions of the multiphase medium, the interfacial continuity conditions between these regions, and the externally applied boundary conditions. This system is solved by an explicit step-by-step procedure in time, and the resulting time-dependent displacement and stress response can be recorded at any point within the multiphase medium. In addition, parts of the discretized geometry may contain fluids. Thus, the air surrounding the multiphase medium can be simulated, with the acoustic loading applied to the air rather than directly on the multiphase panel. This is useful as it more realistically simulated the impact of a pressure wave on the surface of the panel, as wave reflection can be captured. Various cases of porous absorbers can be modeled by employing this theory. Examples include limp absorbers, where the solid ligaments are so thin and compliant that they can be assumed to have near-zero stiffness; rigid absorbers, where the ligaments are so stiff that they can be assumed to be motionless (with very high stiffness); and poroelastic absorbers, where both the ligaments and the air within the considered domain participate in the wave propagation. In the present investigation, the latter case is mainly considered.

Theoretical model development is first presented. Then, results are given for the structural/acoustic performance of several foam core sandwich panels. Finally, heterogeneous panels, consisting of a stiff phase and a very compliant phase, are examined to determine the effect of the arrangement of the phases on the panel acoustic behavior.

Full Three-Dimensional Theory

In the present section a three-dimensional continuum theory is developed for the analysis of wave propagation in multiphase materials. To this end, consider a three-dimensional domain defined by $0 \le x_1 \le D$, $0 \le x_2 \le H$, and $0 \le x_3 \le L$. This region is divided into N_α, N_β and N_γ subcells in the x_1, x_2 and x_3 directions, respectively. Each subcell $(\alpha\beta\gamma)$, whose dimensions are d_α, h_β and l_γ ($\alpha = 1,\ldots, N_\alpha$, $\beta = 1,\ldots, N_\beta$, $\gamma = 1,\ldots N_\gamma$), can be filled by a distinct anisotropic elastic material (solid or fluid) or is left empty thus forming a pore, see Figure 1.

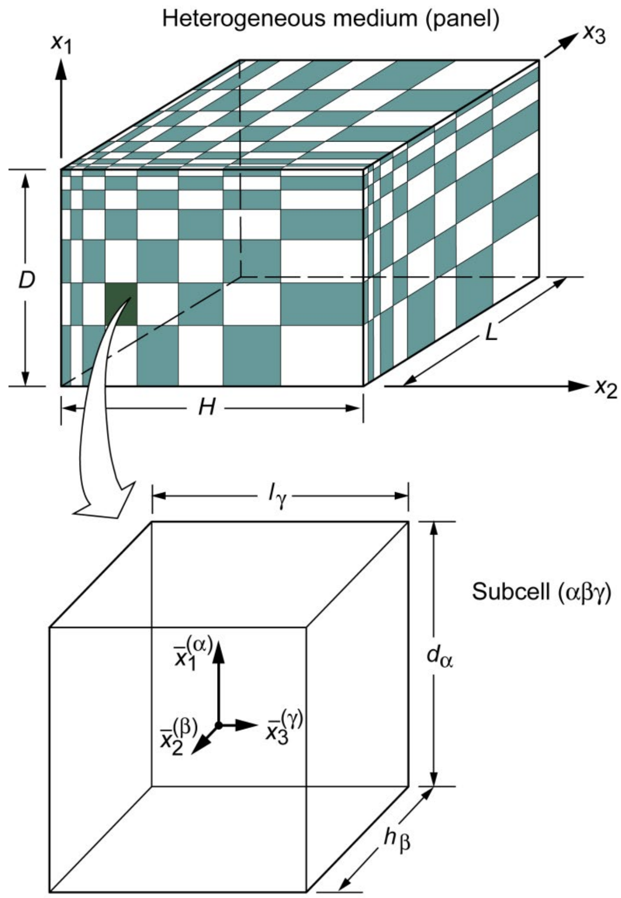

Figure 1.—Model geometry.

The derivation of this theory starts from the elastodynamic equations of motion

$$\sigma_{ji,j}^{(\alpha\beta\gamma)} = \rho^{(\alpha\beta\gamma)} \frac{d^2}{dt^2} u_i^{(\alpha\beta\gamma)}, \qquad i, j = 1,2,3 \tag{1}$$

where $\sigma_{ji}^{(\alpha\beta\gamma)}$, $u_i^{(\alpha\beta\gamma)}$, $\rho^{(\alpha\beta\gamma)}$ and t denote the stresses, displacements, mass density of the material in subcell $(\alpha\beta\gamma)$ and time. The stresses $\sigma_{ij}^{(\alpha\beta\gamma)}$ are related to the strains $\varepsilon_{ij}^{(\alpha\beta\gamma)}$ by the anisotropic Hooke's law

$$\sigma_{ij}^{(\alpha\beta\gamma)} = C_{ijkl}^{(\alpha\beta\gamma)} \varepsilon_{kl}^{(\alpha\beta\gamma)}, \qquad i, j, k, l = 1,2,3 \tag{2}$$

where $C_{ijkl}^{(\alpha\beta\gamma)}$ are the components of the 4th-order stiffness tensor of the material in the subcell.

The displacement field in the subcell $(\alpha\beta\gamma)$ is approximated by a second-order expansion in the local coordinates $\bar{x}_1^{(\alpha)}$, $\bar{x}_2^{(\beta)}$ and $\bar{x}_3^{(\gamma)}$, the origins of which are located at the center of the subcells, as follows:

$$\begin{aligned} u_1^{(\alpha\beta\gamma)} &= W_{1(000)}^{(\alpha\beta\gamma)} + \bar{x}_1^{(\alpha)} W_{1(100)}^{(\alpha\beta\gamma)} + \bar{x}_2^{(\beta)} W_{1(010)}^{(\alpha\beta\gamma)} + \bar{x}_3^{(\gamma)} W_{1(001)}^{(\alpha\beta\gamma)} \\ &+ \frac{1}{2}\left(3\bar{x}_1^{(\alpha)2} - \frac{d_\alpha^2}{4}\right) W_{1(200)}^{(\alpha\beta\gamma)} + \frac{1}{2}\left(3\bar{x}_2^{(\beta)2} - \frac{h_\beta^2}{4}\right) W_{1(020)}^{(\alpha\beta\gamma)} + \frac{1}{2}\left(3\bar{x}_3^{(\gamma)2} - \frac{l_\gamma^2}{4}\right) W_{1(002)}^{(\alpha\beta\gamma)} \end{aligned} \tag{3}$$

$$
\begin{aligned}
u_2^{(\alpha\beta\gamma)} &= W_{2(000)}^{(\alpha\beta\gamma)} + \bar{x}_1^{(\alpha)} W_{2(100)}^{(\alpha\beta\gamma)} + \bar{x}_2^{(\beta)} W_{2(010)}^{(\alpha\beta\gamma)} + \bar{x}_3^{(\gamma)} W_{2(001)}^{(\alpha\beta\gamma)} \\
&+ \frac{1}{2}\left(3\bar{x}_1^{(\alpha)2} - \frac{d_\alpha^2}{4}\right) W_{2(200)}^{(\alpha\beta\gamma)} + \frac{1}{2}\left(3\bar{x}_2^{(\beta)2} - \frac{h_\beta^2}{4}\right) W_{2(020)}^{(\alpha\beta\gamma)} + \frac{1}{2}\left(3\bar{x}_3^{(\gamma)2} - \frac{l_\gamma^2}{4}\right) W_{2(002)}^{(\alpha\beta\gamma)}
\end{aligned}
\tag{4}
$$

$$
\begin{aligned}
u_3^{(\alpha\beta\gamma)} &= W_{3(000)}^{(\alpha\beta\gamma)} + \bar{x}_1^{(\alpha)} W_{3(100)}^{(\alpha\beta\gamma)} + \bar{x}_2^{(\beta)} W_{3(010)}^{(\alpha\beta\gamma)} + \bar{x}_3^{(\gamma)} W_{3(001)}^{(\alpha\beta\gamma)} \\
&+ \frac{1}{2}\left(3\bar{x}_1^{(\alpha)2} - \frac{d_\alpha^2}{4}\right) W_{3(200)}^{(\alpha\beta\gamma)} + \frac{1}{2}\left(3\bar{x}_2^{(\beta)2} - \frac{h_\beta^2}{4}\right) W_{3(020)}^{(\alpha\beta\gamma)} + \frac{1}{2}\left(3\bar{x}_3^{(\gamma)2} - \frac{l_\gamma^2}{4}\right) W_{3(002)}^{(\alpha\beta\gamma)}
\end{aligned}
\tag{5}
$$

where the time-dependent $W_{i(000)}^{(\alpha\beta\gamma)}$, ($i$ = 1,2,3), are the volume-average displacements in the subcell which together with the higher-order time-dependent terms $W_{i(lmn)}^{(\alpha\beta\gamma)}$; ($l$,$m$,$n$) = 1,2; must be determined. Thus, for example, $W_{i(020)}^{(\alpha\beta\gamma)}$ denotes the coefficient in the expansion of $u_i^{(\alpha\beta\gamma)}$ the quadratic term associated with the x_2-direction. The resulting strain components in subcell ($\alpha\beta\gamma$) are given by

$$
\begin{aligned}
\varepsilon_{11}^{(\alpha\beta\gamma)} &= W_{1(100)}^{(\alpha\beta\gamma)} + 3\bar{x}_1^{(\alpha)} W_{1(200)}^{(\alpha\beta\gamma)} \\
\varepsilon_{22}^{(\alpha\beta\gamma)} &= W_{2(010)}^{(\alpha\beta\gamma)} + 3\bar{x}_2^{(\beta)} W_{2(020)}^{(\alpha\beta\gamma)} \\
\varepsilon_{33}^{(\alpha\beta\gamma)} &= W_{3(001)}^{(\alpha\beta\gamma)} + 3\bar{x}_3^{(\gamma)} W_{3(002)}^{(\alpha\beta\gamma)} \\
\varepsilon_{23}^{(\alpha\beta\gamma)} &= \frac{1}{2}\left(W_{2(001)}^{(\alpha\beta\gamma)} + 3\bar{x}_3^{(\gamma)} W_{2(002)}^{(\alpha\beta\gamma)} + W_{3(010)}^{(\alpha\beta\gamma)} + 3\bar{x}_2^{(\beta)} W_{3(020)}^{(\alpha\beta\gamma)}\right) \\
\varepsilon_{13}^{(\alpha\beta\gamma)} &= \frac{1}{2}\left(W_{1(001)}^{(\alpha\beta\gamma)} + 3\bar{x}_3^{(\gamma)} W_{1(002)}^{(\alpha\beta\gamma)} + W_{3(100)}^{(\alpha\beta\gamma)} + 3\bar{x}_1^{(\alpha)} W_{3(200)}^{(\alpha\beta\gamma)}\right) \\
\varepsilon_{12}^{(\alpha\beta\gamma)} &= \frac{1}{2}\left(W_{1(010)}^{(\alpha\beta\gamma)} + 3\bar{x}_2^{(\beta)} W_{1(020)}^{(\alpha\beta\gamma)} + W_{2(100)}^{(\alpha\beta\gamma)} + 3\bar{x}_1^{(\alpha)} W_{2(200)}^{(\alpha\beta\gamma)}\right)
\end{aligned}
\tag{6}
$$

By averaging Equation (1) over the volume of subcell ($\alpha\beta\gamma$), the following three relations are obtained

$$
I_{1i(000)}^{(\alpha\beta\gamma)} + J_{2i(000)}^{(\alpha\beta\gamma)} + K_{3i(000)}^{(\alpha\beta\gamma)} = \rho^{(\alpha\beta\gamma)} \ddot{W}_{i(000)}^{(\alpha\beta\gamma)}, \qquad i = 1,2,3 \tag{7}
$$

where $I_{1i(000)}^{(\alpha\beta\gamma)}$, $J_{2i(000)}^{(\alpha\beta\gamma)}$ and $K_{3i(000)}^{(\alpha\beta\gamma)}$ which were originally introduced by Aboudi (1986, 1987) are given in terms of the surface-average of the tractions evaluated at the surfaces $\bar{y}_1^{(\alpha)} = \pm d_\alpha/2$, $\bar{y}_2^{(\beta)} = \pm h_\beta/2$ and $\bar{y}_3^{(\gamma)} = \pm l_\gamma/2$, respectively. Thus

$$
I_{1i(000)}^{(\alpha\beta\gamma)} = \frac{1}{d_\alpha}\left[\overset{(1)+}{t_i}{}^{(\alpha\beta\gamma)} - \overset{(1)-}{t_i}{}^{(\alpha\beta\gamma)} \right] \tag{8}
$$

$$
J_{2i(000)}^{(\alpha\beta\gamma)} = \frac{1}{h_\beta}\left[\overset{(2)+}{t_i}{}^{(\alpha\beta\gamma)} - \overset{(2)-}{t_i}{}^{(\alpha\beta\gamma)} \right] \tag{9}
$$

$$K_{3i(000)}^{(\alpha\beta\gamma)} = \frac{1}{l_\gamma}\left[\overset{(3)+}{t_i}{}^{(\alpha\beta\gamma)} - \overset{(3)-}{t_i}{}^{(\alpha\beta\gamma)} \right] \tag{10}$$

where the surface-average of the tractions are given by

$$\overset{(1)\pm}{t_i}{}^{(\alpha\beta\gamma)} = \frac{1}{h_\beta l_\gamma}\int_{-h_\beta/2}^{h_\beta/2}\int_{-l_\gamma/2}^{l_\gamma/2} \sigma_{1i}^{(\alpha\beta\gamma)}\left(\bar{x}_1^{(\alpha)} = \pm\frac{d_\alpha}{2} \right) d\bar{x}_2^{(\beta)} d\bar{x}_3^{(\gamma)} \tag{11}$$

$$\overset{(2)\pm}{t_i}{}^{(\alpha\beta\gamma)} = \frac{1}{d_\alpha l_\gamma}\int_{-d_\alpha/2}^{d_\alpha/2}\int_{-l_\gamma/2}^{l_\gamma/2} \sigma_{2i}^{(\alpha\beta\gamma)}\left(\bar{x}_2^{(\beta)} = \pm\frac{h_\beta}{2} \right) d\bar{x}_1^{(\alpha)} d\bar{x}_3^{(\gamma)} \tag{12}$$

$$\overset{(3)\pm}{t_i}{}^{(\alpha\beta\gamma)} = \frac{1}{d_\alpha h_\beta}\int_{-d_\alpha/2}^{d_\alpha/2}\int_{-h_\beta/2}^{h_\beta/2} \sigma_{3i}^{(\alpha\beta\gamma)}\left(\bar{x}_3^{(\gamma)} = \pm\frac{l_\gamma}{2} \right) d\bar{x}_1^{(\alpha)} d\bar{x}_2^{(\beta)} \tag{13}$$

Next, by consecutively multiplying Equation (1) by $\bar{x}_1^{(\alpha)}$, $\bar{x}_2^{(\beta)}$ and $\bar{x}_3^{(\gamma)}$ and averaging the results over the volume of the subcell ($\alpha\beta\gamma$) and integrating by parts, the following three set of three relations follow

$$I_{1i(100)}^{(\alpha\beta\gamma)} - S_{1i(000)}^{(\alpha\beta\gamma)} = \rho^{(\alpha\beta\gamma)}\frac{d_\alpha^2}{12}\ddot{W}_{i(100)}^{(\alpha\beta\gamma)}, \qquad i = 1,2,3 \tag{14}$$

$$J_{2i(010)}^{(\alpha\beta\gamma)} - S_{2i(000)}^{(\alpha\beta\gamma)} = \rho^{(\alpha\beta\gamma)}\frac{h_\beta^2}{12}\ddot{W}_{i(010)}^{(\alpha\beta\gamma)}, \qquad i = 1,2,3 \tag{15}$$

$$K_{3i(001)}^{(\alpha\beta\gamma)} - S_{3i(000)}^{(\alpha\beta\gamma)} = \rho^{(\alpha\beta\gamma)}\frac{l_\gamma^2}{12}\ddot{W}_{i(001)}^{(\alpha\beta\gamma)}, \qquad i = 1,2,3 \tag{16}$$

In these equations, the quantities $I_{1i(100)}^{(\alpha\beta\gamma)}$, $J_{2i(010)}^{(\alpha\beta\gamma)}$ and $K_{3i(001)}^{(\alpha\beta\gamma)}$ can be expressed in terms of the surface-average of tractions as follows

$$I_{1i(100)}^{(\alpha\beta\gamma)} = \frac{1}{2}\left[\overset{(1)+}{t_i}{}^{(\alpha\beta\gamma)} + \overset{(1)-}{t_i}{}^{(\alpha\beta\gamma)} \right] \tag{17}$$

$$J_{2i(010)}^{(\alpha\beta\gamma)} = \frac{1}{2}\left[\overset{(2)+}{t_i}{}^{(\alpha\beta\gamma)} + \overset{(2)-}{t_i}{}^{(\alpha\beta\gamma)} \right] \tag{18}$$

$$K_{3i(001)}^{(\alpha\beta\gamma)} = \frac{1}{2}\left[\overset{(3)+}{t_i}{}^{(\alpha\beta\gamma)} + \overset{(3)-}{t_i}{}^{(\alpha\beta\gamma)} \right] \tag{19}$$

In addition, $S_{ij(000)}^{(\alpha\beta\gamma)}$ denote the volume-average of the stress $\sigma_{ij}^{(\alpha\beta\gamma)}$ over the subcell namely,

$$S_{ij(000)}^{(\alpha\beta\gamma)} = \frac{1}{d_\alpha h_\beta l_\gamma} \int_{-d_\alpha/2}^{d_\alpha/2} \int_{-h_\beta/2}^{h_\beta/2} \int_{-l_\gamma/2}^{l_\gamma/2} \sigma_{ij}^{(\alpha\beta\gamma)} d\bar{x}_1^{(\alpha)} d\bar{x}_2^{(\beta)} d\bar{x}_3^{(\gamma)} \tag{20}$$

Let the vector $\mathbf{S}_{(000)}^{(\alpha\beta\gamma)}$ be defined by the following six components of $S_{ij(000)}^{(\alpha\beta\gamma)}$:

$$\mathbf{S}_{(000)}^{(\alpha\beta\gamma)} = \left[S_{11(000)},\ S_{22(000)},\ S_{33(000)},\ S_{23(000)},\ S_{13(000)},\ S_{12(000)}\right]^{(\alpha\beta\gamma)} \tag{21}$$

In terms of the reduced matrix representation C_{pq}; $p,q = 1,\ldots,6$; of the stiffness tensor C_{ijkl}, it can be easily verified by employing the strain components expressions in Equation (6) that its components are given by

$$\begin{aligned} S_{p(000)}^{(\alpha\beta\gamma)} &= C_{p1}^{(\alpha\beta\gamma)} W_{1(100)}^{(\alpha\beta\gamma)} + C_{p2}^{(\alpha\beta\gamma)} W_{2(010)}^{(\alpha\beta\gamma)} + C_{p3}^{(\alpha\beta\gamma)} W_{3(001)}^{(\alpha\beta\gamma)} + C_{p4}^{(\alpha\beta\gamma)} \left(W_{2(001)}^{(\alpha\beta\gamma)} + W_{3(010)}^{(\alpha\beta\gamma)}\right) \\ &+ C_{p5}^{(\alpha\beta\gamma)} \left(W_{1(001)}^{(\alpha\beta\gamma)} + W_{3(100)}^{(\alpha\beta\gamma)}\right) + C_{p6}^{(\alpha\beta\gamma)} \left(W_{1(010)}^{(\alpha\beta\gamma)} + W_{2(100)}^{(\alpha\beta\gamma)}\right) \end{aligned} \tag{22}$$

Next, by consecutively multiplying Equation (1) by $\bar{x}_1^{2(\alpha)}$, $\bar{x}_2^{2(\beta)}$ and $\bar{x}_3^{2(\gamma)}$ and averaging the result over the volume of the subcell ($\alpha\beta\gamma$) and integrating by parts, the following three set of three relations follow

$$\frac{d_\alpha^2}{4} I_{1i(000)}^{(\alpha\beta\gamma)} + \frac{d_\alpha^2}{12}\left[J_{2i(000)}^{(\alpha\beta\gamma)} + K_{3i(000)}^{(\alpha\beta\gamma)}\right] - 2S_{1i(100)}^{(\alpha\beta\gamma)} = \rho^{(\alpha\beta\gamma)} \frac{d_\alpha^2}{12}\left[\ddot{W}_{i(000)}^{(\alpha\beta\gamma)} + \frac{d_\alpha^2}{10}\ddot{W}_{i(200)}^{(\alpha\beta\gamma)}\right], \quad i = 1,2,3 \tag{23}$$

$$\frac{h_\beta^2}{4} J_{2i(000)}^{(\alpha\beta\gamma)} + \frac{h_\beta^2}{12}\left[I_{1i(000)}^{(\alpha\beta\gamma)} + K_{3i(000)}^{(\alpha\beta\gamma)}\right] - 2S_{2i(010)}^{(\alpha\beta\gamma)} = \rho^{(\alpha\beta\gamma)} \frac{h_\beta^2}{12}\left[\ddot{W}_{i(000)}^{(\alpha\beta\gamma)} + \frac{h_\beta^2}{10}\ddot{W}_{i(020)}^{(\alpha\beta\gamma)}\right], \quad i = 1,2,3 \tag{24}$$

$$\frac{l_\gamma^2}{4} K_{3i(000)}^{(\alpha\beta\gamma)} + \frac{l_\gamma^2}{12}\left[I_{1i(000)}^{(\alpha\beta\gamma)} + J_{2i(000)}^{(\alpha\beta\gamma)}\right] - 2S_{3i(001)}^{(\alpha\beta\gamma)} = \rho^{(\alpha\beta\gamma)} \frac{l_\gamma^2}{12}\left[\ddot{W}_{i(000)}^{(\alpha\beta\gamma)} + \frac{l_\gamma^2}{10}\ddot{W}_{i(002)}^{(\alpha\beta\gamma)}\right], \quad i = 1,2,3 \tag{25}$$

In these equations, $S_{ij(lmn)}^{(\alpha\beta\gamma)}$ are the volume-average first moments of the stresses which are given by

$$S_{ij(lmn)}^{(\alpha\beta\gamma)} = \frac{1}{d_\alpha h_\beta h_\beta} \int_{-d_\alpha/2}^{d_\alpha/2} \int_{-h_\beta/2}^{l_\gamma/2} \int_{-l_\gamma/2}^{l_\gamma/2} \left(\bar{x}_1^{(\alpha)}\right)^l \left(\bar{x}_2^{(\beta)}\right)^m \left(\bar{x}_3^{(\gamma)}\right)^n \sigma_{ij}^{(\alpha\beta\gamma)} d\bar{x}_1^{(\alpha)} d\bar{x}_2^{(\beta)} d\bar{x}_3^{(\gamma)} \tag{26}$$

It can be easily shown that the relevant components of the vector $\mathbf{S}_{(lmn)}^{(\alpha\beta\gamma)}$, $l + m + n \neq 0$, that is defined by

$$\mathbf{S}_{(lmn)}^{(\alpha\beta\gamma)} = \left[S_{11(lmn)},\ S_{22(lmn)},\ S_{33(lmn)},\ S_{23(lmn)},\ S_{13(lmn)},\ S_{12(lmn)}\right]^{(\alpha\beta\gamma)} \tag{27}$$

are given by

$$S_{p(100)}^{(\alpha\beta\gamma)} = \frac{d_\alpha^2}{4}\left[C_{p1}^{(\alpha\beta\gamma)} W_{1(200)}^{(\alpha\beta\gamma)} + C_{p6}^{(\alpha\beta\gamma)} W_{2(200)}^{(\alpha\beta\gamma)} + C_{p5}^{(\alpha\beta\gamma)} W_{3(200)}^{(\alpha\beta\gamma)}\right] \tag{28}$$

$$S_{p(010)}^{(\alpha\beta\gamma)}=\frac{h_\beta^2}{4}\left[C_{p6}^{(\alpha\beta\gamma)}W_{1(020)}^{(\alpha\beta\gamma)}+C_{p2}^{(\alpha\beta\gamma)}W_{2(020)}^{(\alpha\beta\gamma)}+C_{p4}^{(\alpha\beta\gamma)}W_{3(020)}^{(\alpha\beta\gamma)}\right] \tag{29}$$

$$S_{p(001)}^{(\alpha\beta\gamma)}=\frac{l_\gamma^2}{4}\left[C_{p5}^{(\alpha\beta\gamma)}W_{1(002)}^{(\alpha\beta\gamma)}+C_{p4}^{(\alpha\beta\gamma)}W_{2(002)}^{(\alpha\beta\gamma)}+C_{p3}^{(\alpha\beta\gamma)}W_{3(002)}^{(\alpha\beta\gamma)}\right] \tag{30}$$

where $p = 1,\ldots,6$.

By substituting Equations (7) in (23), (24) and (25) one obtains, respectively, that

$$I_{1i(000)}^{(\alpha\beta\gamma)}=\frac{12}{d_\alpha^2}S_{1i(100)}^{(\alpha\beta\gamma)}+\rho^{(\alpha\beta\gamma)}\frac{d_\alpha^2}{20}\ddot{W}_{i(200)}^{(\alpha\beta\gamma)} \tag{31}$$

$$J_{2i(000)}^{(\alpha\beta\gamma)}=\frac{12}{h_\beta^2}S_{2i(010)}^{(\alpha\beta\gamma)}+\rho^{(\alpha\beta\gamma)}\frac{h_\beta^2}{20}\ddot{W}_{i(020)}^{(\alpha\beta\gamma)} \tag{32}$$

$$K_{3i(000)}^{(\alpha\beta\gamma)}=\frac{12}{l_\gamma^2}S_{3i(001)}^{(\alpha\beta\gamma)}+\rho^{(\alpha\beta\gamma)}\frac{l_\gamma^2}{20}\ddot{W}_{i(002)}^{(\alpha\beta\gamma)} \tag{33}$$

Hence substitution of Equations (31) to (33) in (7) yields

$$\frac{12}{d_\alpha^2}S_{1i(100)}^{(\alpha\beta\gamma)}+\frac{12}{h_\beta^2}S_{2i(010)}^{(\alpha\beta\gamma)}+\frac{12}{l_\gamma^2}S_{3i(001)}^{(\alpha\beta\gamma)}=\rho^{(\alpha\beta\gamma)}\left[\ddot{W}_{i(000)}^{(\alpha\beta\gamma)}-\frac{d_\alpha^2}{20}\ddot{W}_{i(200)}^{(\alpha\beta\gamma)}-\frac{h_\beta^2}{20}\ddot{W}_{i(020)}^{(\alpha\beta\gamma)}-\frac{l_\gamma^2}{20}\ddot{W}_{i(002)}^{(\alpha\beta\gamma)}\right] \tag{34}$$

Just like the surface-average of tractions: $\overset{(1)\pm(\alpha\beta\gamma)}{t_i}$, $\overset{(2)\pm(\alpha\beta\gamma)}{t_i}$ and $\overset{(3)\pm(\alpha\beta\gamma)}{t_i}$ which were defined by Equations (11) to (13), let us define the surface-average of displacements: $\overset{(1)\pm(\alpha\beta\gamma)}{u_i}$, $\overset{(2)\pm(\alpha\beta\gamma)}{u_i}$ and $\overset{(3)\pm(\alpha\beta\gamma)}{u_i}$ as follows

$$\overset{(1)\pm(\alpha\beta\gamma)}{u_i}=\frac{1}{h_\beta l_\gamma}\int_{-h_\beta/2}^{h_\beta/2}\int_{-l_\gamma/2}^{l_\gamma/2}u_i^{(\alpha\beta\gamma)}\left(\bar{x}_1^{(\alpha)}=\pm\frac{d_\alpha}{2}\right)d\bar{x}_2^{(\beta)}d\bar{x}_3^{(\gamma)} \tag{35}$$

$$\overset{(2)\pm(\alpha\beta\gamma)}{u_i}=\frac{1}{d_\alpha l_\gamma}\int_{-d_\alpha/2}^{d_\alpha/2}\int_{-l_\gamma/2}^{l_\gamma/2}u_i^{(\alpha\beta\gamma)}\left(\bar{x}_2^{(\beta)}=\pm\frac{h_\beta}{2}\right)d\bar{x}_1^{(\alpha)}d\bar{x}_3^{(\gamma)} \tag{36}$$

$$\overset{(3)\pm(\alpha\beta\gamma)}{u_i}=\frac{1}{d_\alpha h_\beta}\int_{-d_\alpha/2}^{d_\alpha/2}\int_{-h_\beta/2}^{h_\beta/2}u_i^{(\alpha\beta\gamma)}\left(\bar{x}_3^{(\gamma)}=\pm\frac{l_\gamma}{2}\right)d\bar{x}_1^{(\alpha)}d\bar{x}_2^{(\beta)} \tag{37}$$

In the following, these surface-average displacements will be related to the microvariables $W_{i(lmn)}^{(\alpha\beta\gamma)}$; $(lmn) = 0,1,2$; in the displacements expansions. To this end, by substituting the displacements expansion (3) to (5) in (35) to (37), the following relations are obtained

$$\overset{(1)\pm(\alpha\beta\gamma)}{u_i} = W_{i(000)}^{(\alpha\beta\gamma)} \pm \frac{d_\alpha}{2} W_{i(100)}^{(\alpha\beta\gamma)} + \frac{d_\alpha^2}{4} W_{i(200)}^{(\alpha\beta\gamma)} \tag{38}$$

$$\overset{(2)\pm(\alpha\beta\gamma)}{u_i} = W_{i(000)}^{(\alpha\beta\gamma)} \pm \frac{h_\beta}{2} W_{i(010)}^{(\alpha\beta\gamma)} + \frac{h_\beta^2}{4} W_{i(020)}^{(\alpha\beta\gamma)} \tag{39}$$

$$\overset{(3)\pm(\alpha\beta\gamma)}{u_i} = W_{i(000)}^{(\alpha\beta\gamma)} \pm \frac{l_\gamma}{2} W_{i(001)}^{(\alpha\beta\gamma)} + \frac{l_\gamma^2}{4} W_{i(002)}^{(\alpha\beta\gamma)} \tag{40}$$

Subtraction of the pair of two equations in (38), (39) and (40) yields, respectively, that

$$W_{i(100)}^{(\alpha\beta\gamma)} = \frac{1}{d_\alpha}\left[\overset{(1)+(\alpha\beta\gamma)}{u_i} - \overset{(1)-(\alpha\beta\gamma)}{u_i}\right] \tag{41}$$

$$W_{i(010)}^{(\alpha\beta\gamma)} = \frac{1}{h_\beta}\left[\overset{(2)+(\alpha\beta\gamma)}{u_i} - \overset{(2)-(\alpha\beta\gamma)}{u_i}\right] \tag{42}$$

$$W_{i(001)}^{(\alpha\beta\gamma)} = \frac{1}{l_\gamma}\left[\overset{(3)+(\alpha\beta\gamma)}{u_i} - \overset{(3)-(\alpha\beta\gamma)}{u_i}\right] \tag{43}$$

Similarly, adding the pair of two equations in (38), (39) and (40) yields, respectively, that

$$W_{i(200)}^{(\alpha\beta\gamma)} = \frac{2}{d_\alpha^2}\left[\overset{(1)+(\alpha\beta\gamma)}{u_i} + \overset{(1)-(\alpha\beta\gamma)}{u_i}\right] - \frac{4}{d_\alpha^2} W_{i(000)}^{(\alpha\beta\gamma)} \tag{44}$$

$$W_{i(020)}^{(\alpha\beta\gamma)} = \frac{2}{h_\beta^2}\left[\overset{(2)+(\alpha\beta\gamma)}{u_i} + \overset{(2)-(\alpha\beta\gamma)}{u_i}\right] - \frac{4}{h_\beta^2} W_{i(000)}^{(\alpha\beta\gamma)} \tag{45}$$

$$W_{i(002)}^{(\alpha\beta\gamma)} = \frac{2}{l_\gamma^2}\left[\overset{(3)+(\alpha\beta\gamma)}{u_i} + \overset{(3)-(\alpha\beta\gamma)}{u_i}\right] - \frac{4}{l_\gamma^2} W_{i(000)}^{(\alpha\beta\gamma)} \tag{46}$$

Substitution of Equations (44) to (46) in (34) provides the following expression for the second time derivative $\ddot{W}_{i(000)}^{(\alpha\beta\gamma)}$ in terms of the stress moments and the second time derivatives of the surface-average displacements:

$$\ddot{W}^{(\alpha\beta\gamma)}_{i(000)} = \frac{1}{16}\frac{d^2}{dt^2}\left[\overset{(1)+(\alpha\beta\gamma)}{u_i} + \overset{(1)-(\alpha\beta\gamma)}{u_i} + \overset{(2)+(\alpha\beta\gamma)}{u_i} + \overset{(2)-(\alpha\beta\gamma)}{u_i} + \overset{(3)+(\alpha\beta\gamma)}{u_i} + \overset{(3)-(\alpha\beta\gamma)}{u_i}\right] + \frac{15}{2\rho^{(\alpha\beta\gamma)}}\left[\frac{1}{d_\alpha^2}S^{(\alpha\beta\gamma)}_{1i(100)} + \frac{1}{h_\beta^2}S^{(\alpha\beta\gamma)}_{2i(010)} + \frac{1}{l_\gamma^2}S^{(\alpha\beta\gamma)}_{3i(001)}\right] \tag{47}$$

Similarly, the expressions for $\ddot{W}^{(\alpha\beta\gamma)}_{i(200)}$, $\ddot{W}^{(\alpha\beta\gamma)}_{i(020)}$ and $\ddot{W}^{(\alpha\beta\gamma)}_{i(002)}$ can be obtained by substituting Equation (47) in (44) to (46) yielding respectively

$$\ddot{W}^{(\alpha\beta\gamma)}_{i(200)} = \frac{1}{4d_\alpha^2}\frac{d^2}{dt^2}\left[7\left(\overset{(1)+(\alpha\beta\gamma)}{u_i} + \overset{(1)-(\alpha\beta\gamma)}{u_i}\right) - \overset{(2)+(\alpha\beta\gamma)}{u_i} - \overset{(2)-(\alpha\beta\gamma)}{u_i} - \overset{(3)+(\alpha\beta\gamma)}{u_i} - \overset{(3)-(\alpha\beta\gamma)}{u_i}\right] - \frac{30}{\rho^{(\alpha\beta\gamma)}d_\alpha^2}\left[\frac{1}{d_\alpha^2}S^{(\alpha\beta\gamma)}_{1i(100)} + \frac{1}{h_\beta^2}S^{(\alpha\beta\gamma)}_{2i(010)} + \frac{1}{l_\gamma^2}S^{(\alpha\beta\gamma)}_{3i(001)}\right] \tag{48}$$

$$\ddot{W}^{(\alpha\beta\gamma)}_{i(020)} = \frac{1}{4h_\beta^2}\frac{d^2}{dt^2}\left[-\overset{(1)+(\alpha\beta\gamma)}{u_i} - \overset{(1)-(\alpha\beta\gamma)}{u_i} + 7\left(\overset{(2)+(\alpha\beta\gamma)}{u_i} + \overset{(2)-(\alpha\beta\gamma)}{u_i}\right) - \overset{(3)+(\alpha\beta\gamma)}{u_i} - \overset{(3)-(\alpha\beta\gamma)}{u_i}\right] - \frac{30}{\rho^{(\alpha\beta\gamma)}h_\beta^2}\left[\frac{1}{d_\alpha^2}S^{(\alpha\beta\gamma)}_{1i(100)} + \frac{1}{h_\beta^2}S^{(\alpha\beta\gamma)}_{2i(010)} + \frac{1}{l_\gamma^2}S^{(\alpha\beta\gamma)}_{3i(001)}\right] \tag{49}$$

$$\ddot{W}^{(\alpha\beta\gamma)}_{i(002)} = \frac{1}{4l_\gamma^2}\frac{d^2}{dt^2}\left[-\overset{(1)+(\alpha\beta\gamma)}{u_i} - \overset{(1)-(\alpha\beta\gamma)}{u_i} - \overset{(2)+(\alpha\beta\gamma)}{u_i} - \overset{(2)-(\alpha\beta\gamma)}{u_i} + 7\left(\overset{(3)+(\alpha\beta\gamma)}{u_i} + \overset{(3)-(\alpha\beta\gamma)}{u_i}\right)\right] - \frac{30}{\rho^{(\alpha\beta\gamma)}l_\gamma^2}\left[\frac{1}{d_\alpha^2}S^{(\alpha\beta\gamma)}_{1i(100)} + \frac{1}{h_\beta^2}S^{(\alpha\beta\gamma)}_{2i(010)} + \frac{1}{l_\gamma^2}S^{(\alpha\beta\gamma)}_{3i(001)}\right] \tag{50}$$

With the established values of $\ddot{W}^{(\alpha\beta\gamma)}_{i(lmn)}$ given above in terms of the second-order time derivatives of the surface-average displacements and volume-average stress, moments one can proceed and express the values of $I^{(\alpha\beta\gamma)}_{1i(lmn)}$, $J^{(\alpha\beta\gamma)}_{2i(lmn)}$ and $K^{(\alpha\beta\gamma)}_{3i(lmn)}$ in these terms as follows. Equations (31) and (14), (32) and (15) and (33) and (16) provide, respectively, that

$$I^{(\alpha\beta\gamma)}_{1i(000)} = \frac{\rho^{(\alpha\beta\gamma)}}{80}\frac{d^2}{dt^2}\left[7\left(\overset{(1)+(\alpha\beta\gamma)}{u_i} + \overset{(1)-(\alpha\beta\gamma)}{u_i}\right) - \overset{(2)+(\alpha\beta\gamma)}{u_i} - \overset{(2)-(\alpha\beta\gamma)}{u_i} - \overset{(3)+(\alpha\beta\gamma)}{u_i} - \overset{(3)-(\alpha\beta\gamma)}{u_i}\right] + \frac{21}{2d_\alpha^2}S^{(\alpha\beta\gamma)}_{1i(100)} - \frac{3}{2h_\beta^2}S^{(\alpha\beta\gamma)}_{2i(010)} - \frac{3}{2l_\gamma^2}S^{(\alpha\beta\gamma)}_{3i(001)} \tag{51}$$

$$I^{(\alpha\beta\gamma)}_{1i(100)} = \frac{\rho^{(\alpha\beta\gamma)}d_\alpha}{12}\frac{d^2}{dt^2}\left[\overset{(1)+(\alpha\beta\gamma)}{u_i} - \overset{(1)-(\alpha\beta\gamma)}{u_i}\right] + S^{(\alpha\beta\gamma)}_{1i(000)} \tag{52}$$

$$
\begin{aligned}
J_{2i(000)}^{(\alpha\beta\gamma)} = {} & \frac{\rho^{(\alpha\beta\gamma)}}{80}\frac{d^2}{dt^2}\left[-\overset{(1)+(\alpha\beta\gamma)}{u_i} - \overset{(1)-(\alpha\beta\gamma)}{u_i} + 7\left(\overset{(2)+(\alpha\beta\gamma)}{u_i} + \overset{(2)-(\alpha\beta\gamma)}{u_i}\right) - \overset{(3)+(\alpha\beta\gamma)}{u_i} - \overset{(3)-(\alpha\beta\gamma)}{u_i}\right] \\
& - \frac{3}{2d_\alpha^2}S_{1i(100)}^{(\alpha\beta\gamma)} + \frac{21}{2h_\beta^2}S_{2i(010)}^{(\alpha\beta\gamma)} - \frac{3}{2l_\gamma^2}S_{3i(001)}^{(\alpha\beta\gamma)}
\end{aligned} \tag{53}
$$

$$
J_{2i(010)}^{(\alpha\beta\gamma)} = \frac{\rho^{(\alpha\beta\gamma)}h_\beta}{12}\frac{d^2}{dt^2}\left[\overset{(2)+(\alpha\beta\gamma)}{u_i} - \overset{(2)-(\alpha\beta\gamma)}{u_i}\right] + S_{2i(000)}^{(\alpha\beta\gamma)} \tag{54}
$$

and

$$
\begin{aligned}
K_{3i(000)}^{(\alpha\beta\gamma)} = {} & \frac{\rho^{(\alpha\beta\gamma)}}{80}\frac{d^2}{dt^2}\left[-\overset{(1)+(\alpha\beta\gamma)}{u_i} - \overset{(1)-(\alpha\beta\gamma)}{u_i} - \overset{(2)+(\alpha\beta\gamma)}{u_i} - \overset{(2)-(\alpha\beta\gamma)}{u_i} + 7\left(\overset{(3)+(\alpha\beta\gamma)}{u_i} + \overset{(3)-(\alpha\beta\gamma)}{u_i}\right)\right] \\
& - \frac{3}{2d_\alpha^2}S_{1i(100)}^{(\alpha\beta\gamma)} - \frac{3}{2h_\beta^2}S_{2i(010)}^{(\alpha\beta\gamma)} + \frac{21}{2l_\gamma^2}S_{3i(001)}^{(\alpha\beta\gamma)}
\end{aligned} \tag{55}
$$

$$
K_{3i(001)}^{(\alpha\beta\gamma)} = \frac{\rho^{(\alpha\beta\gamma)}l_\gamma}{12}\frac{d^2}{dt^2}\left[\overset{(3)+(\alpha\beta\gamma)}{u_i} - \overset{(3)-(\alpha\beta\gamma)}{u_i}\right] + S_{3i(000)}^{(\alpha\beta\gamma)} \tag{56}
$$

From Equations (8) to (10) and (17) to (19), the surface-average tractions can be obtained as

$$
\overset{(1)\pm(\alpha\beta\gamma)}{t_i} = \pm\frac{d_\alpha}{2}I_{1i(000)}^{(\alpha\beta\gamma)} + I_{1i(100)}^{(\alpha\beta\gamma)} \tag{57}
$$

$$
\overset{(2)\pm(\alpha\beta\gamma)}{t_i} = \pm\frac{h_\beta}{2}J_{2i(000)}^{(\alpha\beta\gamma)} + J_{2i(010)}^{(\alpha\beta\gamma)} \tag{58}
$$

$$
\overset{(3)\pm(\alpha\beta\gamma)}{t_i} = \pm\frac{l_\gamma}{2}K_{3i(000)}^{(\alpha\beta\gamma)} + K_{3i(001)}^{(\alpha\beta\gamma)} \tag{59}
$$

Hence, it is possible to express these surface-average tractions in terms of the second-order time derivatives of the surface-average displacements and volume-average stresses and stress moments by substituting in Equations (57) to (59) the expression of $I_{1i(lmn)}^{(\alpha\beta\gamma)}$, $J_{2i(lmn)}^{(\alpha\beta\gamma)}$ and $K_{3i(lmn)}^{(\alpha\beta\gamma)}$ which are given by Equations (51) to (56) yielding

$$
\begin{aligned}
\overset{(1)\pm(\alpha\beta\gamma)}{t_i} = {} & \\
& \pm\frac{\rho^{(\alpha\beta\gamma)}d_\alpha}{160}\frac{d^2}{dt^2}\left[7\left(\overset{(1)+(\alpha\beta\gamma)}{u_i} + \overset{(1)-(\alpha\beta\gamma)}{u_i}\right) + \overset{(2)+(\alpha\beta\gamma)}{u_i} - \overset{(2)-(\alpha\beta\gamma)}{u_i} - \overset{(3)+(\alpha\beta\gamma)}{u_i} - \overset{(3)-(\alpha\beta\gamma)}{u_i}\right] \\
& + \frac{\rho^{(\alpha\beta\gamma)}d_\alpha}{12}\frac{d^2}{dt^2}\left[\overset{(1)+(\alpha\beta\gamma)}{u_i} - \overset{(1)-(\alpha\beta\gamma)}{u_i}\right] \pm \left[\frac{21}{4d_\alpha}S_{1i(100)}^{(\alpha\beta\gamma)} - \frac{3d_\alpha}{4h_\beta^2}S_{2i(010)}^{(\alpha\beta\gamma)} - \frac{3d_\alpha}{4l_\gamma^2}S_{3i(001)}^{(\alpha\beta\gamma)}\right] + S_{1i(000)}^{(\alpha\beta\gamma)}
\end{aligned} \tag{60}
$$

$$
\begin{aligned}
\overset{(2)\pm(\alpha\beta\gamma)}{t_i} =\; & \\
& \pm\frac{\rho^{(\alpha\beta\gamma)}h_\beta}{160}\frac{d^2}{dt^2}\left[-\overset{(1)+(\alpha\beta\gamma)}{u_i}-\overset{(1)-(\alpha\beta\gamma)}{u_i}+7\left(\overset{(2)+(\alpha\beta\gamma)}{u_i}+\overset{(2)-(\alpha\beta\gamma)}{u_i}\right)-\overset{(3)+(\alpha\beta\gamma)}{u_i}-\overset{(3)-(\alpha\beta\gamma)}{u_i}\right] \\
& +\frac{\rho^{(\alpha\beta\gamma)}h_\beta}{12}\frac{d^2}{dt^2}\left[\overset{(2)+(\alpha\beta\gamma)}{u_i}-\overset{(2)-(\alpha\beta\gamma)}{u_i}\right]\pm\left[-\frac{3h_\beta}{4d_\alpha^2}S_{1i(100)}^{(\alpha\beta\gamma)}+\frac{21}{4h_\beta}S_{2i(010)}^{(\alpha\beta\gamma)}-\frac{3h_\beta}{4l_\gamma^2}S_{3i(001)}^{(\alpha\beta\gamma)}\right]+S_{2i(000)}^{(\alpha\beta\gamma)}
\end{aligned}
\tag{61}
$$

$$
\begin{aligned}
\overset{(3)\pm(\alpha\beta\gamma)}{t_i} =\; & \\
& \pm\frac{\rho^{(\alpha\beta\gamma)}l_\gamma}{160}\frac{d^2}{dt^2}\left[-\overset{(1)+(\alpha\beta\gamma)}{u_i}-\overset{(1)-(\alpha\beta\gamma)}{u_i}-\overset{(2)+(\alpha\beta\gamma)}{u_i}-\overset{(2)-(\alpha\beta\gamma)}{u_i}+7\left(\overset{(3)+(\alpha\beta\gamma)}{u_i}+\overset{(3)-(\alpha\beta\gamma)}{u_i}\right)\right] \\
& +\frac{\rho^{(\alpha\beta\gamma)}l_\gamma}{12}\frac{d^2}{dt^2}\left[\overset{(3)+(\alpha\beta\gamma)}{u_i}-\overset{(3)-(\alpha\beta\gamma)}{u_i}\right]\pm\left[-\frac{3l_\gamma}{4d_\alpha^2}S_{1i(100)}^{(\alpha\beta\gamma)}-\frac{3l_\gamma}{4h_\beta^2}S_{2i(010)}^{(\alpha\beta\gamma)}+\frac{21}{4l_\gamma}S_{3i(001)}^{(\alpha\beta\gamma)}\right]+S_{3i(000)}^{(\alpha\beta\gamma)}
\end{aligned}
\tag{62}
$$

Equations (60) to (62) can be written in the compact form

$$
\begin{Bmatrix}
\overset{(1)+}{t_1}\\ \overset{(1)-}{t_1}\\ \overset{(1)+}{t_2}\\ \overset{(1)-}{t_2}\\ \overset{(1)+}{t_3}\\ \overset{(1)-}{t_3}\\
\overset{(2)+}{t_1}\\ \overset{(2)-}{t_1}\\ \overset{(2)+}{t_2}\\ \overset{(2)-}{t_2}\\ \overset{(2)+}{t_3}\\ \overset{(2)-}{t_3}\\
\overset{(3)+}{t_1}\\ \overset{(3)-}{t_1}\\ \overset{(3)+}{t_2}\\ \overset{(3)-}{t_2}\\ \overset{(3)+}{t_3}\\ \overset{(3)-}{t_3}
\end{Bmatrix}^{(\alpha\beta\gamma)}
=\left[K\right]^{(\alpha\beta\gamma)}\frac{d^2}{dt^2}
\begin{Bmatrix}
\overset{(1)+}{u_1}\\ \overset{(1)-}{u_1}\\ \overset{(1)+}{u_2}\\ \overset{(1)-}{u_2}\\ \overset{(1)+}{u_3}\\ \overset{(1)-}{u_3}\\
\overset{(2)+}{u_1}\\ \overset{(2)-}{u_1}\\ \overset{(2)+}{u_2}\\ \overset{(2)-}{u_2}\\ \overset{(2)+}{u_3}\\ \overset{(2)-}{u_3}\\
\overset{(3)+}{u_1}\\ \overset{(3)-}{u_1}\\ \overset{(3)+}{u_2}\\ \overset{(3)-}{u_2}\\ \overset{(3)+}{u_3}\\ \overset{(3)-}{u_3}
\end{Bmatrix}^{(\alpha\beta\gamma)}
+\left[L\right]^{(\alpha\beta\gamma)}
\begin{Bmatrix}
S_{11(000)}\\ S_{12(000)}\\ S_{13(000)}\\ S_{21(000)}\\ S_{22(000)}\\ S_{23(000)}\\ S_{31(000)}\\ S_{32(000)}\\ S_{33(000)}\\
S_{11(100)}\\ S_{12(100)}\\ S_{13(100)}\\ S_{21(010)}\\ S_{22(010)}\\ S_{23(010)}\\ S_{31(001)}\\ S_{32(001)}\\ S_{33(001)}
\end{Bmatrix}^{(\alpha\beta\gamma)}
\tag{63}
$$

where $\alpha = 1,\ldots, N_\alpha$; $\beta = 1,\ldots, N_\beta$; $\gamma = 1,\ldots N_\gamma$ and $K^{(\alpha\beta\gamma)}$ is a 18×18 matrix whose elements depend on the dimensions of the subcell ($\alpha\beta\gamma$) and the properties of the material filling this subcell, whereas $L^{(\alpha\beta\gamma)}$ is a matrix of the same dimensions whose elements depend on the dimensions of the subcell.

The continuity of the interfacial tractions between neighboring subcells implies that

$$\overset{(1)+(\alpha\beta\gamma)}{t_i} = \overset{(1)-(\alpha+1,\beta,\gamma)}{t_i}, \quad i = 1,2,3, \quad \alpha = 1,\ldots,N_\alpha - 1, \quad \beta = 1,\ldots N_\beta, \quad \gamma = 1,\ldots,N_\gamma \tag{64}$$

$$\overset{(3)+(\alpha\beta\gamma)}{t_i} = \overset{(3)-(\alpha,\beta,\gamma+1)}{t_i}, \quad i = 1,2,3, \quad \alpha = 1,\ldots,N_\alpha, \quad \beta = 1,\ldots,N_\beta, \quad \gamma = 1,\ldots,N_\gamma - 1 \tag{65}$$

$$\overset{(3)+(\alpha\beta\gamma)}{t_i} = \overset{(3)-(\alpha,\beta,\gamma+1)}{t_i}, \quad i = 1,2,3, \quad \alpha = 1,\ldots,N_\alpha, \quad \beta = 1,\ldots,N_\beta, \quad \gamma = 1,\ldots,N_\gamma - 1 \tag{66}$$

In addition, the continuity of the displacements at the interfaces of the subcells yields

$$\overset{(1)+(\alpha\beta\gamma)}{u_i} = \overset{(1)-(\alpha+1,\beta,\gamma)}{u_i}, \quad i = 1,2,3, \quad \alpha = 1,\ldots,N_\alpha - 1, \quad \beta = 1,\ldots N_\beta, \quad \gamma = 1,\ldots,N_\gamma \tag{67}$$

$$\overset{(2)+(\alpha\beta\gamma)}{u_i} = \overset{(2)-(\alpha,\beta+1,\gamma)}{u_i}, \quad i = 1,2,3, \quad \alpha = 1,\ldots,N_\alpha, \quad \beta = 1,\ldots,N_\beta - 1, \quad \gamma = 1,\ldots,N_\gamma \tag{68}$$

$$\overset{(3)+(\alpha\beta\gamma)}{u_i} = \overset{(3)-(\alpha,\beta,\gamma+1)}{u_i}, \quad i = 1,2,3, \quad \alpha = 1,\ldots,N_\alpha, \quad \beta = 1,\ldots,N_\beta, \quad \gamma = 1,\ldots,N_\gamma - 1 \tag{69}$$

For imperfect bonding between the interfaces, Equations (67) to (69) take the form

$$\begin{gathered}\overset{(1)+(\alpha\beta\gamma)}{u_i} - \overset{(1)-(\alpha+1,\beta,\gamma)}{u_i} - R_{1i}^{(\alpha\beta\gamma)}(t)\,\overset{(1)+(\alpha\beta\gamma)}{t_i} = 0,\\ i = 1,2,3, \quad \alpha = 1,\ldots,N_\alpha - 1, \quad \beta = 1,\ldots N_\beta, \quad \gamma = 1,\ldots,N_\gamma\end{gathered} \tag{70}$$

$$\begin{gathered}\overset{(2)+(\alpha\beta\gamma)}{u_i} - \overset{(2)-(\alpha,\beta+1,\gamma)}{u_i} - R_{2i}^{(\alpha\beta\gamma)}(t)\,\overset{(2)+(\alpha\beta\gamma)}{t_i} = 0,\\ i = 1,2,3, \quad \alpha = 1,\ldots,N_\alpha, \quad \beta = 1,\ldots,N_\beta - 1, \quad \gamma = 1,\ldots,N_\gamma\end{gathered} \tag{71}$$

$$\begin{gathered}\overset{(3)+(\alpha\beta\gamma)}{u_i} - \overset{(3)-(\alpha,\beta,\gamma+1)}{u_i} - R_{3i}^{(\alpha\beta\gamma)}(t)\,\overset{(3)+(\alpha\beta\gamma)}{t_i} = 0,\\ i = 1,2,3, \quad \alpha = 1,\ldots,N_\alpha, \quad \beta = 1,\ldots N_\beta, \quad \gamma = 1,\ldots,N_\gamma - 1\end{gathered} \tag{72}$$

where $R_{1i}^{(\alpha\beta\gamma)}(t)$, $R_{2i}^{(\alpha\beta\gamma)}(t)$ and $R_{3i}^{(\alpha\beta\gamma)}(t)$ denote the time depending debonding functions that describe the behavior of the interfacial debonding of the subcell in the three directions. Wave propagation with imperfect bonding between the phases has been previously investigated by Aboudi (1988a). Not that, in the presence of perfect bonding, these functions are identically zero.

Next, the following time-dependent boundary conditions must be imposed depending on whether the tractions or displacements are prescribed at the surfaces of the subcells at $x_1 = 0$, $x_1 = D$; $x_2 = 0$, $x_2 = H$ and $x_3 = 0$, $x_3 = L$.

$$\overset{(1)\,-(1\beta\gamma)}{t_i} = f_i^{(1)}\left(\bar{x}_2^{(\beta)}, \bar{x}_3^{(\gamma)}, t\right), \quad \text{or} \quad \overset{(1)\,-(1\beta\gamma)}{u_i} = f_i^{(1)}\left(\bar{x}_2^{(\beta)}, \bar{x}_3^{(\gamma)}, t\right),$$
$$i = 1,2,3, \quad \beta = 1,\ldots N_\beta, \quad \gamma = 1,\ldots, N_\gamma \tag{73}$$

and

$$\overset{(1)\,+(N_\alpha\beta\gamma)}{t_i} = g_i^{(1)}\left(\bar{x}_2^{(\beta)}, \bar{x}_3^{(\gamma)}, t\right), \quad \text{or} \quad \overset{(1)\,+(N_\alpha\beta\gamma)}{u_i} = g_i^{(1)}\left(\bar{x}_2^{(\beta)}, \bar{x}_3^{(\gamma)}, t\right),$$
$$i = 1,2,3, \quad \beta = 1,\ldots N_\beta, \quad \gamma = 1,\ldots, N_\gamma \tag{74}$$

$$\overset{(2)\,-(\alpha 1\gamma)}{t_i} = f_i^{(2)}\left(\bar{x}_1^{(\alpha)}, \bar{x}_3^{(\gamma)}, t\right), \quad \text{or} \quad \overset{(2)\,-(\alpha 1\gamma)}{u_i} = f_i^{(2)}\left(\bar{x}_1^{(\alpha)}, \bar{x}_3^{(\gamma)}, t\right),$$
$$i = 1,2,3, \quad \alpha = 1,\ldots N_\alpha, \quad \gamma = 1,\ldots, N_\gamma \tag{75}$$

and

$$\overset{(2)\,+(\alpha N_\beta\gamma)}{t_i} = g_i^{(2)}\left(\bar{x}_1^{(\alpha)}, \bar{x}_3^{(\gamma)}, t\right), \quad \text{or} \quad \overset{(2)\,+(\alpha N_\beta\gamma)}{u_i} = g_i^{(2)}\left(\bar{x}_1^{(\alpha)}, \bar{x}_3^{(\gamma)}, t\right),$$
$$i = 1,2,3, \quad \alpha = 1,\ldots N_\alpha, \quad \gamma = 1,\ldots, N_\gamma \tag{76}$$

Finally,

$$\overset{(3)\,-(\alpha\beta 1)}{t_i} = f_i^{(3)}\left(\bar{x}_1^{(\alpha)}, \bar{x}_2^{(\beta)}, t\right), \quad \text{or} \quad \overset{(3)\,-(\alpha\beta 1)}{u_i} = f_i^{(3)}\left(\bar{x}_1^{(\alpha)}, \bar{x}_2^{(\beta)}, t\right),$$
$$i = 1,2,3, \quad \alpha = 1,\ldots N_\alpha, \quad \beta = 1,\ldots, N_\beta \tag{77}$$

and

$$\overset{(3)\,+(\alpha\beta N_\gamma)}{t_i} = g_i^{(3)}\left(\bar{x}_1^{(\alpha)}, \bar{x}_2^{(\beta)}, t\right), \quad \text{or} \quad \overset{(3)\,+(\alpha\beta N_\gamma)}{u_i} = g_i^{(3)}\left(\bar{x}_1^{(\alpha)}, \bar{x}_2^{(\beta)}, t\right),$$
$$i = 1,2,3, \quad \alpha = 1,\ldots N_\alpha, \quad \beta = 1,\ldots, N_\beta \tag{78}$$

In these equations, $f_i^{(k)}$ and $g_i^{(k)}$, i,k = 1,2,3, are time-dependent functions that describe the temporal form of the various applied loadings at the specific locations of boundaries of the region.

There are $18N_\alpha N_\beta N_\gamma$ unknowns $\frac{d^2}{dt^2}\overset{(1)\,\pm(\alpha\beta\gamma)}{u_i}$, $\frac{d^2}{dt^2}\overset{(2)\,\pm(\alpha\beta\gamma)}{u_i}$, $\frac{d^2}{dt^2}\overset{(3)\,\pm(\alpha\beta\gamma)}{u_i}$, i = 1,2,3. On the other hand, the interfacial traction and displacement provide $6(N_\alpha N_\beta N_\gamma - N_\beta N_\gamma)$, $6(N_\alpha N_\beta N_\gamma - N_\alpha N_\gamma)$ and $6(N_\alpha N_\beta N_\gamma - N_\alpha N_\beta)$ which are respectively given by Equations (64) and (67) (or (70)), (65) and (68) (or (71)), and (66) and (69) (or (72)). In addition, the boundary conditions (73) and (74), (75) and (76) and (77) and (78) form another $6N_\beta N_\gamma$, $6N_\alpha N_\gamma$ and $6N_\alpha N_\beta$ relations, respectively. Thus the total number of equations is $18N_\alpha N_\beta N_\gamma$.

The resulting system of the $18N_\alpha N_\beta N_\gamma$ equations can be formally represented by

$$\mathbf{A}\ddot{\mathbf{X}}(t) = \mathbf{B}(t) \tag{79}$$

where **A** is a matrix of dimension $18N_\alpha N_\beta N_\gamma \times 18N_\alpha N_\beta N_\gamma$ whose elements are the material parameters and geometric dimensions, and $\mathbf{B}(t)$ consists of time-dependent elements that involve the stresses and the imposed boundary conditions at time t. This equation represents the entire multiphase medium that result from filling the subcells with various types of elastic materials (including pores and fluids). It also represents the elastodynamic equations that govern the motion of the material within the subcells, the various interfacial conditions between the subcells, and the applied time-dependent boundary conditions.

A central finite difference of a second order accuracy in the time increment Δt reduces this ordinary differential equation to the following explicit form

$$\mathbf{X}(t+\Delta t) = 2\mathbf{X}(t) - \mathbf{X}(t-\Delta t) + (\Delta t)^2 \mathbf{A}^{-1}\mathbf{B}(t) \tag{80}$$

from which the variables can be computed at time $t + \Delta t$ from their known values at times t and $t - \Delta t$. This procedure is continued to the next time increment. Stability of this finite difference procedure is ensured by a proper choice of the value of the time increment Δt. It should be noted that in the analysis of porous materials, the tractions at the walls of the empty subcell are equal to zero, so that the number of equations can be reduced by excluding this type of subcell from the system of equations.

In the special case of multi-layered composites, the accuracy of the model was verified by comparison with the ray theory prediction (Aboudi, 1988b). Furthermore, in this latter special situation of multi-layered composites, extensive applications and verifications of the accuracy of the model were recently presented by Clements et al. (1996, 1997a, 1997b, 1998) including comparisons with measured data. In addition, these authors introduced more developments and made more refinements to the model. Also, the analysis of harmonic wave propagation in laminated composites was presented by Aboudi and Hevroni (1991).

Specialization to Two-Dimensional Theory for Thermoelastic Panels

Consider the case of two-dimensional wave propagation such that there is no dependence of any field variable on the direction x_1. This situation corresponds to the case in which the direction of the propagating waves is perpendicular to the x_1-direction. For example, wave propagation in fiber reinforced materials in which the waves propagate in the perpendicular direction to the continuous fibers can be analyzed by present two-dimensional theory. Wave propagation in a panel in the through-thickness direction can be analyzed by the present two-dimensional theory for wave traveling in the x_2-direction.

In this two-dimensional theory all variables depend only on the x_2- and x_3-directions, in addition to the time, t. The plane x_2–x_3 is divided this time into $N_\beta \times N_\gamma$ subcells with $\beta = 1,\ldots, N_\beta$, $\gamma = 1,\ldots N_\gamma$. In addition, $\bar{x}_2^{(\beta)}$ and $\bar{x}_3^{(\beta)}$ are local coordinates whose origin is located at the center of the subcell $(\beta\gamma)$, see Figure 2. Hence the displacement expansions, Equations (3) to (5), reduce in this special case to

$$\begin{aligned} u_1^{(\beta\gamma)} &= W_{1(00)}^{(\beta\gamma)} + \bar{x}_2^{(\beta)} W_{1(10)}^{(\beta\gamma)} + \bar{x}_3^{(\gamma)} W_{1(01)}^{(\beta\gamma)} \\ &\quad + \frac{1}{2}\left(3\bar{x}_2^{(\beta)2} - \frac{h_\beta^2}{4}\right) W_{1(20)}^{(\beta\gamma)} + \frac{1}{2}\left(3\bar{x}_3^{(\gamma)2} - \frac{l_\gamma^2}{4}\right) W_{1(02)}^{(\beta\gamma)} \end{aligned} \tag{1}$$

$$\begin{aligned} u_2^{(\beta\gamma)} &= W_{2(00)}^{(\beta\gamma)} + \bar{x}_2^{(\beta)} W_{2(10)}^{(\beta\gamma)} + \bar{x}_3^{(\gamma)} W_{2(01)}^{(\beta\gamma)} \\ &\quad + \frac{1}{2}\left(3\bar{x}_2^{(\beta)2} - \frac{h_\beta^2}{4}\right) W_{2(20)}^{(\beta\gamma)} + \frac{1}{2}\left(3\bar{x}_3^{(\gamma)2} - \frac{l_\gamma^2}{4}\right) W_{2(02)}^{(\beta\gamma)} \end{aligned} \tag{2}$$

$$\begin{aligned} u_3^{(\beta\gamma)} &= W_{3(00)}^{(\beta\gamma)} + \bar{x}_2^{(\beta)} W_{3(10)}^{(\beta\gamma)} + \bar{x}_3^{(\gamma)} W_{3(01)}^{(\beta\gamma)} \\ &\quad + \frac{1}{2}\left(3\bar{x}_2^{(\beta)2} - \frac{h_\beta^2}{4}\right) W_{3(20)}^{(\beta\gamma)} + \frac{1}{2}\left(3\bar{x}_3^{(\gamma)2} - \frac{l_\gamma^2}{4}\right) W_{3(02)}^{(\beta\gamma)} \end{aligned} \tag{3}$$

The resulting strain components in subcell (βγ) are given by

$$
\begin{aligned}
\varepsilon_{11}^{(\beta\gamma)} &= 0 \\
\varepsilon_{22}^{(\beta\gamma)} &= W_{2(10)}^{(\beta\gamma)} + 3\bar{x}_2^{(\beta)} W_{2(20)}^{(\beta\gamma)} \\
\varepsilon_{33}^{(\beta\gamma)} &= W_{3(01)}^{(\beta\gamma)} + 3\bar{x}_3^{(\gamma)} W_{3(02)}^{(\beta\gamma)} \\
\varepsilon_{23}^{(\beta\gamma)} &= \frac{1}{2}\left(W_{2(01)}^{(\beta\gamma)} + 3\bar{x}_3^{(\gamma)} W_{2(02)}^{(\beta\gamma)} + W_{3(10)}^{(\beta\gamma)} + 3\bar{x}_2^{(\beta)} W_{3(20)}^{(\beta\gamma)}\right) \\
\varepsilon_{13}^{(\beta\gamma)} &= \frac{1}{2}\left(W_{1(01)}^{(\beta\gamma)} + 3\bar{x}_3^{(\gamma)} W_{1(02)}^{(\beta\gamma)}\right) \\
\varepsilon_{12}^{(\beta\gamma)} &= \frac{1}{2}\left(W_{1(10)}^{(\beta\gamma)} + 3\bar{x}_2^{(\beta)} W_{1(20)}^{(\beta\gamma)}\right)
\end{aligned} \tag{4}
$$

The governing equations that correspond to Equations (7), (15) and (16) are given by

$$J_{2i(00)}^{(\beta\gamma)} + K_{3i(00)}^{(\beta\gamma)} = \rho^{(\beta\gamma)} \ddot{W}_{i(00)}^{(\beta\gamma)}, \qquad i = 1,2,3 \tag{5}$$

$$J_{2i(10)}^{(\beta\gamma)} - S_{2i(00)}^{(\beta\gamma)} = \rho^{(\beta\gamma)} \frac{h_\beta^2}{12} \ddot{W}_{i(10)}^{(\beta\gamma)}, \qquad i = 1,2,3 \tag{6}$$

$$K_{3i(01)}^{(\beta\gamma)} - S_{3i(00)}^{(\beta\gamma)} = \rho^{(\beta\gamma)} \frac{l_\gamma^2}{12} \ddot{W}_{i(01)}^{(\beta\gamma)}, \qquad i = 1,2,3 \tag{7}$$

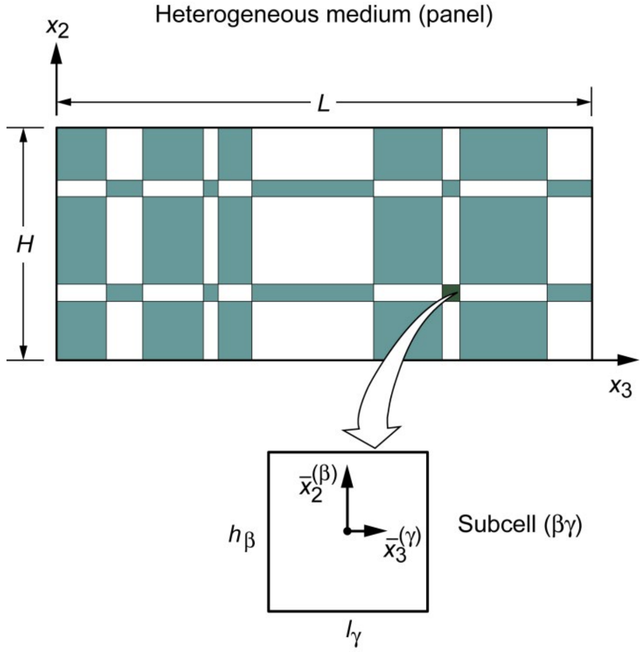

Figure 2.—Geometry of the model specialized to two dimensions.

Here $J^{(\beta\gamma)}_{2i(mn)}$ and $K^{(\beta\gamma)}_{3i(mn)}$ are related to the surface-average tractions in the following manner

$$J^{(\beta\gamma)}_{2i(00)} = \frac{1}{h_\beta}\left[\overset{(2)+(\beta\gamma)}{t_i} - \overset{(2)-(\beta\gamma)}{t_i} \right] \tag{8}$$

$$K^{(\beta\gamma)}_{3i(00)} = \frac{1}{l_\gamma}\left[\overset{(3)+(\beta\gamma)}{t_i} - \overset{(3)-(\beta\gamma)}{t_i} \right] \tag{9}$$

and

$$J^{(\beta\gamma)}_{2i(10)} = \frac{1}{2}\left[\overset{(2)+(\beta\gamma)}{t_i} + \overset{(2)-(\beta\gamma)}{t_i} \right] \tag{10}$$

$$K^{(\beta\gamma)}_{3i(01)} = \frac{1}{2}\left[\overset{(3)+(\beta\gamma)}{t_i} + \overset{(3)-(\beta\gamma)}{t_i} \right] \tag{11}$$

where the surface-average tractions are given by

$$\overset{(2)\pm(\beta\gamma)}{t_i} = \frac{1}{l_\gamma}\int_{-l_\gamma/2}^{l_\gamma/2} \sigma^{(\beta\gamma)}_{2i}\left(\bar{x}^{(\beta)}_2 = \pm\frac{h_\beta}{2} \right) d\bar{x}^{(\gamma)}_3 \tag{12}$$

$$\overset{(3)\pm(\beta\gamma)}{t_i} = \frac{1}{h_\beta}\int_{-h_\beta/2}^{h_\beta/2} \sigma^{(\beta\gamma)}_{3i}\left(\bar{x}^{(\gamma)}_3 = \pm\frac{l_\gamma}{2} \right) d\bar{x}^{(\beta)}_2 \tag{13}$$

Furthermore, the volume-average stresses and stress moments are given by

$$S^{(\beta\gamma)}_{ij(mn)} = \frac{1}{h_\beta l_\gamma}\int_{-h_\beta/2}^{h_\beta/2}\int_{-l_\gamma/2}^{l_\gamma/2} \left(\bar{x}^{(\beta)}_2\right)^m \left(\bar{x}^{(\gamma)}_3\right)^n \sigma^{(\beta\gamma)}_{ij} d\bar{x}^{(\beta)}_2 d\bar{x}^{(\gamma)}_3, \qquad i,j = 1,2,3 \tag{14}$$

Let

$$\mathbf{S}^{(\beta\gamma)}_{(mn)} = \left[S_{11(mn)},\ S_{22(mn)},\ S_{33(mn)},\ S_{23(mn)},\ S_{13(mn)},\ S_{12(mn)} \right]^{(\beta\gamma)} \tag{15}$$

In conjunction with strain components Equations (4), (14) yields

$$S^{(\beta\gamma)}_{p(00)} = C^{(\beta\gamma)}_{p2} W^{(\beta\gamma)}_{2(10)} + C^{(\beta\gamma)}_{p3} W^{(\beta\gamma)}_{3(01)} + C^{(\beta\gamma)}_{p4}\left(W^{(\beta\gamma)}_{2(01)} + W^{(\beta\gamma)}_{3(10)} \right) + C^{(\beta\gamma)}_{p5} W^{(\beta\gamma)}_{1(01)} + C^{(\beta\gamma)}_{p6} W^{(\beta\gamma)}_{1(10)} - \Gamma^{(\beta\gamma)}_p \theta \tag{16}$$

$$S^{(\beta\gamma)}_{p(10)} = \frac{h_\beta^2}{4}\left[C^{(\beta\gamma)}_{p6} W^{(\beta\gamma)}_{1(20)} + C^{(\beta\gamma)}_{p2} W^{(\beta\gamma)}_{2(20)} + C^{(\beta\gamma)}_{p4} W^{(\beta\gamma)}_{3(20)} \right] \tag{17}$$

$$S_{p(01)}^{(\beta\gamma)} = \frac{l_\gamma^2}{4}\left[C_{p5}^{(\beta\gamma)} W_{1(02)}^{(\beta\gamma)} + C_{p4}^{(\beta\gamma)} W_{2(02)}^{(\beta\gamma)} + C_{p3}^{(\beta\gamma)} W_{3(02)}^{(\beta\gamma)}\right] \tag{18}$$

where $p = 1,\ldots,6$ and $\Gamma_p^{(\beta\gamma)}$ are the components of the thermal stresses and θ is the temperature deviation from a reference temperature, T_R.

The two equations that correspond to Equations (24) and (25) are presently given by

$$\frac{h_\beta^2}{4} J_{2i(00)}^{(\beta\gamma)} + \frac{h_\beta^2}{12}\left[K_{3i(00)}^{(\beta\gamma)}\right] - 2S_{2i(10)}^{(\beta\gamma)} = \rho^{(\beta\gamma)} \frac{h_\beta^2}{12}\left[\ddot{W}_{i(00)}^{(\beta\gamma)} + \frac{h_\beta^2}{10}\ddot{W}_{i(20)}^{(\beta\gamma)}\right], \qquad i = 1,2,3 \tag{19}$$

$$\frac{l_\gamma^2}{4} K_{3i(00)}^{(\beta\gamma)} + \frac{l_\gamma^2}{12}\left[J_{2i(00)}^{(\beta\gamma)}\right] - 2S_{3i(01)}^{(\beta\gamma)} = \rho^{(\beta\gamma)} \frac{l_\gamma^2}{12}\left[\ddot{W}_{i(00)}^{(\beta\gamma)} + \frac{l_\gamma^2}{10}\ddot{W}_{i(02)}^{(\beta\gamma)}\right], \qquad i = 1,2,3 \tag{20}$$

Hence by substituting Equation (5) in these two equations, the following relations (that correspond to Equations (32) and (33)) can be presently established

$$J_{2i(00)}^{(\beta\gamma)} = \frac{12}{h_\beta^2} S_{2i(10)}^{(\beta\gamma)} + \rho^{(\beta\gamma)} \frac{h_\beta^2}{20}\ddot{W}_{i(20)}^{(\beta\gamma)} \tag{21}$$

$$K_{3i(00)}^{(\beta\gamma)} = \frac{12}{l_\gamma^2} S_{3i(01)}^{(\beta\gamma)} + \rho^{(\beta\gamma)} \frac{l_\gamma^2}{20}\ddot{W}_{i(02)}^{(\beta\gamma)} \tag{22}$$

Hence, substituting Equations (21) and (22) in (5) yields

$$\frac{12}{h_\beta^2} S_{2i(10)}^{(\beta\gamma)} + \frac{12}{l_\gamma^2} S_{3i(01)}^{(\beta\gamma)} = \rho^{(\beta\gamma)}\left[\ddot{W}_{i(00)}^{(\beta\gamma)} - \frac{h_\beta^2}{20}\ddot{W}_{i(20)}^{(\beta\gamma)} - \frac{l_\gamma^2}{20}\ddot{W}_{i(02)}^{(\beta\gamma)}\right] \tag{23}$$

The surface-average displacements $\overset{(2)\pm(\beta\gamma)}{u_i}$ and $\overset{(3)\pm(\beta\gamma)}{u_i}$ are defined by

$$\overset{(2)\pm(\beta\gamma)}{u_i} = \frac{1}{l_\gamma}\int_{-l_\gamma/2}^{l_\gamma/2} u_i^{(\beta\gamma)}\left(\bar{x}_2^{(\beta)} = \pm\frac{h_\beta}{2}\right) d\bar{x}_3^{(\gamma)} \tag{24}$$

$$\overset{(3)\pm(\beta\gamma)}{u_i} = \frac{1}{h_\beta}\int_{-h_\beta/2}^{h_\beta/2} u_i^{(\beta\gamma)}\left(\bar{x}_3^{(\gamma)} = \pm\frac{l_\gamma}{2}\right) d\bar{x}_2^{(\beta)} \tag{25}$$

Substitution of the displacement expansions (1) to (3) in Equations (24) and (25) reveals that these surface-average displacements are related to the microvariables $W_{i(mn)}^{(\beta\gamma)}$ as follows

$$\overset{(2)\pm(\beta\gamma)}{u_i} = W_{i(00)}^{(\beta\gamma)} \pm \frac{h_\beta}{2} W_{i(10)}^{(\beta\gamma)} + \frac{h_\beta^2}{4} W_{i(20)}^{(\beta\gamma)} \tag{26}$$

$$\overset{(3)\pm(\beta\gamma)}{u_i} = W_{i(00)}^{(\beta\gamma)} \pm \frac{l_\gamma}{2} W_{i(01)}^{(\beta\gamma)} + \frac{l_\gamma^2}{4} W_{i(02)}^{(\beta\gamma)} \tag{27}$$

Manipulation of every pair in these equations results in the following

$$W_{i(10)}^{(\beta\gamma)} = \frac{1}{h_\beta}\left[\overset{(2)+(\beta\gamma)}{u_i} - \overset{(2)-(\beta\gamma)}{u_i}\right] \tag{28}$$

$$W_{i(01)}^{(\beta\gamma)} = \frac{1}{l_\gamma}\left[\overset{(3)+(\beta\gamma)}{u_i} - \overset{(3)-(\beta\gamma)}{u_i}\right] \tag{29}$$

$$W_{i(20)}^{(\beta\gamma)} = \frac{2}{h_\beta^2}\left[\overset{(2)+(\beta\gamma)}{u_i} + \overset{(2)-(\beta\gamma)}{u_i}\right] - \frac{4}{h_\beta^2} W_{i(00)}^{(\beta\gamma)} \tag{30}$$

$$W_{i(02)}^{(\beta\gamma)} = \frac{2}{l_\gamma^2}\left[\overset{(3)+(\beta\gamma)}{u_i} + \overset{(3)-(\beta\gamma)}{u_i}\right] - \frac{4}{l_\gamma^2} W_{i(00)}^{(\beta\gamma)} \tag{31}$$

Substitution of Equations (30) and (31) in (23) yields

$$\ddot{W}_{i(00)}^{(\beta\gamma)} = \frac{1}{14}\frac{d^2}{dt^2}\left[\overset{(2)+(\beta\gamma)}{u_i} + \overset{(2)-(\beta\gamma)}{u_i} + \overset{(3)+(\beta\gamma)}{u_i} + \overset{(3)-(\beta\gamma)}{u_i}\right] + \frac{60}{7\rho^{(\beta\gamma)}}\left[\frac{1}{h_\beta^2} S_{2i(10)}^{(\beta\gamma)} + \frac{1}{l_\gamma^2} S_{3i(01)}^{(\beta\gamma)}\right] \tag{32}$$

Consequently, Equations (28) to (31) establish the following expressions

$$\ddot{W}_{i(20)}^{(\beta\gamma)} = \frac{2}{7h_\beta^2}\frac{d^2}{dt^2}\left[6\left(\overset{(2)+(\beta\gamma)}{u_i} + \overset{(2)-(\beta\gamma)}{u_i}\right) - \overset{(3)+(\beta\gamma)}{u_i} - \overset{(3)-(\beta\gamma)}{u_i}\right] - \frac{240}{7\rho^{(\beta\gamma)} h_\beta^2}\left[\frac{1}{h_\beta^2} S_{2i(10)}^{(\beta\gamma)} + \frac{1}{l_\gamma^2} S_{3i(01)}^{(\beta\gamma)}\right] \tag{33}$$

$$\ddot{W}_{i(02)}^{(\beta\gamma)} = \frac{2}{7l_\gamma^2}\frac{d^2}{dt^2}\left[-\overset{(2)+(\beta\gamma)}{u_i} - \overset{(2)-(\beta\gamma)}{u_i} + 6\left(\overset{(3)+(\beta\gamma)}{u_i} + \overset{(3)-(\beta\gamma)}{u_i}\right)\right] - \frac{240}{7\rho^{(\beta\gamma)} l_\gamma^2}\left[\frac{1}{h_\beta^2} S_{2i(10)}^{(\beta\gamma)} + \frac{1}{l_\gamma^2} S_{3i(01)}^{(\beta\gamma)}\right] \tag{34}$$

With the established values of $\ddot{W}_{i(mn)}^{(\beta\gamma)}$, one obtains from Equations (21) and (6) that

$$J_{2i(00)}^{(\beta\gamma)} = \frac{\rho^{(\beta\gamma)}}{70}\frac{d^2}{dt^2}\left[6\left(\overset{(2)+(\beta\gamma)}{u_i} + \overset{(2)-(\beta\gamma)}{u_i}\right) - \overset{(3)+(\beta\gamma)}{u_i} - \overset{(3)-(\beta\gamma)}{u_i}\right] + \frac{72}{7h_\beta^2} S_{2i(10)}^{(\beta\gamma)} - \frac{12}{7l_\gamma^2} S_{3i(01)}^{(\beta\gamma)} \tag{35}$$

and

$$J_{2i(10)}^{(\beta\gamma)} = \frac{\rho^{(\beta\gamma)} h_\beta}{12} \frac{d^2}{dt^2} \left[\overset{(2)+(\beta\gamma)}{u_i} - \overset{(2)-(\beta\gamma)}{u_i} \right] + S_{2i(00)}^{(\beta\gamma)} \tag{36}$$

Similarly, Equations (22) and (7) result in

$$K_{3i(00)}^{(\beta\gamma)} = \frac{\rho^{(\beta\gamma)}}{70} \frac{d^2}{dt^2} \left[- \overset{(2)+(\beta\gamma)}{u_i} - \overset{(2)-(\beta\gamma)}{u_i} + 6 \left(\overset{(3)+(\beta\gamma)}{u_i} + \overset{(3)-(\beta\gamma)}{u_i} \right) \right] - \frac{12}{7h_\beta^2} S_{2i(10)}^{(\beta\gamma)} + \frac{72}{7l_\gamma^2} S_{3i(01)}^{(\beta\gamma)} \tag{37}$$

and

$$K_{3i(01)}^{(\beta\gamma)} = \frac{\rho^{(\beta\gamma)} l_\gamma}{12} \frac{d^2}{dt^2} \left[\overset{(3)+(\beta\gamma)}{u_i} - \overset{(3)-(\beta\gamma)}{u_i} \right] + S_{3i(00)}^{(\beta\gamma)} \tag{38}$$

From Equations (8) to (11), the surface-average tractions can be obtained as

$$\overset{(2)\pm(\beta\gamma)}{t_i} = \pm \frac{h_\beta}{2} J_{2i(00)}^{(\beta\gamma)} + J_{2i(10)}^{(\beta\gamma)} \tag{39}$$

$$\overset{(3)\pm(\beta\gamma)}{t_i} = \pm \frac{l_\gamma}{2} K_{3i(00)}^{(\beta\gamma)} + K_{3i(01)}^{(\beta\gamma)} \tag{40}$$

Consequently, Equations (35) to (38) yield that

$$\begin{aligned} \overset{(2)\pm(\beta\gamma)}{t_i} &= \pm \frac{\rho^{(\beta\gamma)} h_\beta}{140} \frac{d^2}{dt^2} \left[6 \left(\overset{(2)+(\beta\gamma)}{u_i} + \overset{(2)-(\beta\gamma)}{u_i} \right) - \overset{(3)+(\beta\gamma)}{u_i} - \overset{(3)-(\beta\gamma)}{u_i} \right] \\ &+ \frac{\rho^{(\beta\gamma)} h_\beta}{12} \frac{d^2}{dt^2} \left[\overset{(2)+(\beta\gamma)}{u_i} - \overset{(2)-(\beta\gamma)}{u_i} \right] \pm \left[\frac{36}{7h_\beta} S_{2i(10)}^{(\beta\gamma)} - \frac{6h_\beta}{7l_\gamma^2} S_{3i(01)}^{(\beta\gamma)} \right] + S_{2i(00)}^{(\beta\gamma)} \end{aligned} \tag{41}$$

and

$$\begin{aligned} \overset{(3)\pm(\beta\gamma)}{t_i} &= \pm \frac{\rho^{(\beta\gamma)} l_\gamma}{140} \frac{d^2}{dt^2} \left[- \overset{(2)+(\beta\gamma)}{u_i} - \overset{(2)-(\beta\gamma)}{u_i} + 6 \left(\overset{(3)+(\beta\gamma)}{u_i} + \overset{(3)-(\beta\gamma)}{u_i} \right) \right] \\ &+ \frac{\rho^{(\beta\gamma)} l_\gamma}{12} \frac{d^2}{dt^2} \left[\overset{(3)+(\beta\gamma)}{u_i} - \overset{(3)-(\beta\gamma)}{u_i} \right] \pm \left[- \frac{6l_\gamma}{7h_\beta^2} S_{2i(10)}^{(\beta\gamma)} + \frac{36}{7l_\gamma} S_{3i(01)}^{(\beta\gamma)} \right] + S_{3i(00)}^{(\beta\gamma)} \end{aligned} \tag{42}$$

These two sets of 12 equations provide the desired relations between the surface-average tractions and the second-order time derivatives of the surface-average displacements and the volume-average stresses and stress moments.

These equations can summarized in the compact form

$$
\left\{\begin{matrix} \overset{(2)+}{t_1} \\ \overset{(2)-}{t_1} \\ \overset{(2)+}{t_2} \\ \overset{(2)-}{t_2} \\ \overset{(2)+}{t_3} \\ \overset{(2)-}{t_3} \\ \overset{(3)+}{t_1} \\ \overset{(3)-}{t_1} \\ \overset{(3)+}{t_2} \\ \overset{(3)-}{t_2} \\ \overset{(3)+}{t_3} \\ \overset{(3)-}{t_3} \end{matrix}\right\}^{(\beta\gamma)} = \left[K_1\right]^{(\beta\gamma)} \frac{d^2}{dt^2} \left\{\begin{matrix} \overset{(2)+}{u_1} \\ \overset{(2)-}{u_1} \\ \overset{(2)+}{u_2} \\ \overset{(2)-}{u_2} \\ \overset{(2)+}{u_3} \\ \overset{(2)-}{u_3} \\ \overset{(3)+}{u_1} \\ \overset{(3)-}{u_1} \\ \overset{(3)+}{u_2} \\ \overset{(3)-}{u_2} \\ \overset{(3)+}{u_3} \\ \overset{(3)-}{u_3} \end{matrix}\right\}^{(\beta\gamma)} + \left[L_1\right]^{(\beta\gamma)} \left\{\begin{matrix} S_{21(00)} \\ S_{22(00)} \\ S_{23(00)} \\ S_{31(00)} \\ S_{32(00)} \\ S_{33(00)} \\ S_{21(10)} \\ S_{22(10)} \\ S_{23(10)} \\ S_{31(01)} \\ S_{32(01)} \\ S_{33(01)} \end{matrix}\right\}^{(\beta\gamma)} \tag{43}
$$

where $\beta = 1,\ldots, N_\beta$, $\gamma = 1,\ldots N_\gamma$ and $[K_1]^{(\beta\gamma)}$ is a 12×12 matrix whose elements depend on the dimensions of the subcell $(\beta\gamma)$ and the properties of the material filling this subcell, whereas $[L_1]^{(\beta\gamma)}$ is a matrix of the same dimensions whose elements depend on the dimensions of the subcell. In the present two-dimensional case there are $12N_\beta N_\gamma$ unknown surface-average displacements $\overset{(2)\pm}{u_i}{}^{(\beta\gamma)}$ and $\overset{(3)\pm}{u_i}{}^{(\beta\gamma)}$.

The interfacial traction and displacements (assuming perfect bonding) between the subcells are

$$
\overset{(2)+}{t_i}{}^{(\beta\gamma)} = \overset{(2)-}{t_i}{}^{(\beta+1,\gamma)}, \quad i = 1,2,3, \quad \beta = 1,\ldots, N_\beta - 1, \quad \gamma = 1,\ldots, N_\gamma \tag{44}
$$

$$
\overset{(3)+}{t_i}{}^{(\beta\gamma)} = \overset{(3)-}{t_i}{}^{(\beta,\gamma+1)}, \quad i = 1,2,3, \quad \beta = 1,\ldots, N_\beta, \quad \gamma = 1,\ldots, N_\gamma - 1 \tag{45}
$$

and

$$
\overset{(2)+}{u_i}{}^{(\beta\gamma)} = \overset{(2)-}{u_i}{}^{(\beta+1,\gamma)}, \quad i = 1,2,3, \quad \beta = 1,\ldots, N_\beta - 1, \quad \gamma = 1,\ldots, N_\gamma \tag{46}
$$

$$
\overset{(3)+}{u_i}{}^{(\beta\gamma)} = \overset{(3)-}{u_i}{}^{(\beta,\gamma+1)}, \quad i = 1,2,3, \quad \beta = 1,\ldots, N_\beta, \quad \gamma = 1,\ldots, N_\gamma - 1 \tag{47}
$$

Finally, the boundary conditions at $x_2 = 0$ and $x_2 = H$ are

$$
\overset{(2)-}{t_i}{}^{(1\gamma)} = f_i^{(2)}\left(\bar{x}_3^{(\gamma)}, t\right), \quad \text{or} \quad \overset{(2)-}{u_i}{}^{(1\gamma)} = f_i^{(2)}\left(\bar{x}_3^{(\gamma)}, t\right), \quad i = 1,2,3, \quad \gamma = 1,\ldots, N_\gamma \tag{48}
$$

and

$$\overset{(2)+(N\beta\gamma)}{t_i} = g_i^{(2)}\left(\bar{x}_3^{(\gamma)},t\right), \quad \text{or} \quad \overset{(2)+(N\beta\gamma)}{u_i} = g_i^{(2)}\left(\bar{x}_3^{(\gamma)},t\right), \qquad (49)$$
$$i=1,2,3, \quad \gamma=1,\ldots,N_\gamma$$

At $x_3 = 0$ and $x_3 = L$ the boundary conditions are

$$\overset{(3)-(\beta 1)}{t_i} = f_i^{(3)}\left(\bar{x}_2^{(\beta)},t\right), \quad \text{or} \quad \overset{(3)-(\beta 1)}{u_i} = f_i^{(3)}\left(\bar{x}_2^{(\beta)},t\right), \qquad (50)$$
$$i=1,2,3, \quad \beta=1,\ldots,N_\beta$$

and

$$\overset{(3)+(\beta N_\gamma)}{t_i} = g_i^{(3)}\left(\bar{x}_2^{(\beta)},t\right), \quad \text{or} \quad \overset{(3)+(\beta N_\gamma)}{u_i} = g_i^{(3)}\left(\bar{x}_2^{(\beta)},t\right), \qquad (51)$$
$$i=1,2,3, \quad \beta=1,\ldots,N_\beta$$

In summary, just like the three-dimensional continuum theory, the interfacial tractions, Equations (44) and (45), and displacements, Equations (46) and (47), continuity conditions as well as the boundary conditions, Equations (48) to (51), provide the requested system of equations, given by Equation (79), of $12N_\beta N_\gamma$ equations to be solved at any time yielding the surface-average displacements at that time.

Extension to Inelastic Constituent Materials

It is possible to analyze and model wave propagation in inelastic composites. Here it is assumed that the applied impact is sufficiently strong enough to cause the inelastic material to exhibit inelastic flow. To this end, the constitutive equation of the material filling subcell ($\alpha\beta\gamma$) is given instead of Equation (2) by

$$\sigma_{ij}^{(\alpha\beta\gamma)} = C_{ijkl}^{(\alpha\beta\gamma)}\left[\varepsilon_{kl}^{(\alpha\beta\gamma)} - \varepsilon_{kl}^{I(\alpha\beta\gamma)}\right], \quad i,j,k,l=1,2,3 \qquad (1)$$

where $\varepsilon_{ij}^{I(\alpha\beta\gamma)}$ are the inelastic strain components. It is assumed that the inelasticity is governed by an isotropic flow rule. Thus for plasticity, the evolution equation of $\varepsilon_{ij}^{I(\alpha\beta\gamma)}$ is given by

$$\dot{\varepsilon}_{ij}^{I(\alpha\beta\gamma)} = \dot{\Lambda}^{(\alpha\beta\gamma)}\sigma_{ij}^{(\alpha\beta\gamma)} \qquad (2)$$

where $\dot{\Lambda}^{(\alpha\beta\gamma)}$ is the proportionality function. For viscoplastic constituents, the flow rule is given by

$$\dot{\varepsilon}_{ij}^{I(\alpha\beta\gamma)} = \Lambda^{(\alpha\beta\gamma)}\sigma_{ij}^{(\alpha\beta\gamma)} \qquad (3)$$

Since the inelastic flow rule of the inelastic phase is isotropic, it must be that the stiffness tensor $C_{ijkl}^{(\alpha\beta\gamma)}$ of the material is isotropic as well, namely

$$C_{ijkl}^{(\alpha\beta\gamma)} = \lambda^{(\alpha\beta\gamma)}\delta_{ij}\delta_{kl} + \mu^{(\alpha\beta\gamma)}\left(\delta_{ik}\delta_{jl} + \delta_{il}\delta_{jk}\right) \qquad (4)$$

where $\lambda^{(\alpha\beta\gamma)}$ and $\mu^{(\alpha\beta\gamma)}$ are the Lame' constants of the material.

With the isotropic assumption of the inelastic flow rule, Equation (1) implies that

$$\sigma_{ij}^{(\alpha\beta\gamma)} = C_{ijkl}^{(\alpha\beta\gamma)}\varepsilon_{kl}^{(\alpha\beta\gamma)} - 2\mu^{(\alpha\beta\gamma)}\varepsilon_{ij}^{I(\alpha\beta\gamma)} \tag{5}$$

In the perfectly elastic case, the quadratic displacement expansions, Equations (3) to (5), produce linear variation in strains and stresses at each point within a given subcell. In the presence of inelastic effects, however, a linear strain field generated by these expansions does not imply the linearity of the stress field due to the path-dependent deformation. Thus the displacement field microvariables must depend implicitly on the inelastic strain distributions, giving rise to a higher-order stress field than the linear strain field generated from the assumed displacement field representation. In the presence of inelastic effects, this higher order stress field is represented by a higher order Legendre polynomial expansion in the local coordinates. Therefore, the strain field generated from the assumed displacement field, and the resulting mechanical stress field, must be expressed in terms of Legendre polynomials as

$$\varepsilon_{ij}^{(\alpha\beta\gamma)} = \sum_{l=0}^{\infty}\sum_{m=0}^{\infty}\sum_{n=0}^{\infty}\Gamma_{lmn} e_{ij(lmn)}^{(\alpha\beta\gamma)} P_l\left(\zeta_1^{(\alpha)}\right)P_m\left(\zeta_2^{(\beta)}\right)P_n\left(\zeta_3^{(\gamma)}\right) \tag{6}$$

$$\sigma_{ij}^{(\alpha\beta\gamma)} = \sum_{l=0}^{\infty}\sum_{m=0}^{\infty}\sum_{n=0}^{\infty}\Gamma_{lmn} \tau_{ij(lmn)}^{(\alpha\beta\gamma)} P_l\left(\zeta_1^{(\alpha)}\right)P_m\left(\zeta_2^{(\beta)}\right)P_n\left(\zeta_3^{(\gamma)}\right) \tag{7}$$

where $\Gamma_{lmn} = \sqrt{(2l+1)(2m+1)(2n+1)}$, and the nondimensionalized variables ζ_i's defined in the interval $-1 \le \zeta_i \le 1$, are given in terms of the local subcell coordinates as $\zeta_1^{(\alpha)} = \bar{x}^{(\alpha)}/(d_\alpha/2)$, $\zeta_2^{(\beta)} = \bar{x}^{(\beta)}/(h_\beta/2)$, $\zeta_3^{(\gamma)} = \bar{x}^{(\gamma)}/(l_\gamma/2)$.

For the given displacement field representation the upper limits on the summation in the strains expansion (6) becomes 1. The upper limits on the summations in the stresses expansion (7) on the other hand are chosen so that an accurate representation of the stress fields is obtained within each subcell, which depends on the amount of inelastic flow. The coefficients $e_{ij(lmn)}^{(\alpha\beta\gamma)}$ and $\tau_{ij(lmn)}^{(\alpha\beta\gamma)}$ in the above expansions are determined as follows.

The strain coefficients $e_{ij(lmn)}^{(\alpha\beta\gamma)}$ are explicitly determined in terms of the displacement field microvariables using orthogonal properties of Legendre polynomials. For example $e_{ij(000)}^{(\alpha\beta\gamma)} = W_{1(100)}^{(\alpha\beta\gamma)}$ and $e_{ij(100)}^{(\alpha\beta\gamma)} = \sqrt{3}d_\alpha W_{1(200)}^{(\alpha\beta\gamma)}/2$.

The stress coefficients $\tau_{ij(lmn)}^{(\alpha\beta\gamma)}$ are expressed in terms of strain coefficients and the unknown inelastic strain distributions by first substituting the Legendre polynomial representations for $\varepsilon_{ij}^{(\alpha\beta\gamma)}$ and $\sigma_{ij}^{(\alpha\beta\gamma)}$ into the constitutive equations and then utilizing the orthogonality of Legendre polynomials as

$$\tau_{ij(lmn)}^{(\alpha\beta\gamma)} = C_{ijko}^{(\alpha\beta\gamma)} e_{ko(lmn)}^{(\alpha\beta\gamma)} - R_{ij(lmn)}^{(\alpha\beta\gamma)} \tag{8}$$

The $R_{ij(lmn)}^{(\alpha\beta\gamma)}$ terms represent inelastic stress distributions and are calculated in the following manner:

$$R_{ij(lmn)}^{(\alpha\beta\gamma)} = \mu_{((\alpha\beta\gamma)}\frac{\Gamma_{lmn}}{4}\int_{-1}^{1}\int_{-1}^{1}\int_{-1}^{1}\varepsilon_{ij}^{I(\alpha\beta\gamma)} P_l\left(\zeta_1^{(\alpha)}\right)P_m\left(\zeta_2^{(\beta)}\right)P_n\left(\zeta_3^{(\gamma)}\right)d\zeta_1^{(\alpha)}d\zeta_2^{(\beta)}d\zeta_3^{(\gamma)} \tag{9}$$

With the above expression, the volume-average stresses and stress moments $S_{ij(lmn)}^{(\alpha\beta\gamma)}$ in the present case of inelastic constituents can be readily evaluated by employing Equation (26) in conjunction with (7) to (9). This yields the following expressions which respectively replace Equations (22) and (28) to (30):

$$\begin{aligned} S_{p(000)}^{(\alpha\beta\gamma)} &= C_{p1}^{(\alpha\beta\gamma)} W_{1(100)}^{(\alpha\beta\gamma)} + C_{p2}^{(\alpha\beta\gamma)} W_{2(010)}^{(\alpha\beta\gamma)} + C_{p3}^{(\alpha\beta\gamma)} W_{3(001)}^{(\alpha\beta\gamma)} + C_{p4}^{(\alpha\beta\gamma)} \left(W_{2(001)}^{(\alpha\beta\gamma)} + W_{3(010)}^{(\alpha\beta\gamma)} \right) \\ &+ C_{p5}^{(\alpha\beta\gamma)} \left(W_{1(001)}^{(\alpha\beta\gamma)} + W_{3(100)}^{(\alpha\beta\gamma)} \right) + C_{p6}^{(\alpha\beta\gamma)} \left(W_{1(010)}^{(\alpha\beta\gamma)} + W_{2(100)}^{(\alpha\beta\gamma)} \right) - R_{p(000)}^{(\alpha\beta\gamma)} \end{aligned} \tag{10}$$

$$S_{p(100)}^{(\alpha\beta\gamma)} = \frac{d_\alpha^2}{4} \left[C_{p1}^{(\alpha\beta\gamma)} W_{1(200)}^{(\alpha\beta\gamma)} + C_{p6}^{(\alpha\beta\gamma)} W_{2(200)}^{(\alpha\beta\gamma)} + C_{p5}^{(\alpha\beta\gamma)} W_{3(200)}^{(\alpha\beta\gamma)} \right] - \frac{d_\alpha}{2\sqrt{3}} R_{p(100)}^{(\alpha\beta\gamma)} \tag{11}$$

$$S_{p(010)}^{(\alpha\beta\gamma)} = \frac{h_\beta^2}{4} \left[C_{p6}^{(\alpha\beta\gamma)} W_{1(020)}^{(\alpha\beta\gamma)} + C_{p2}^{(\alpha\beta\gamma)} W_{2(020)}^{(\alpha\beta\gamma)} + C_{p4}^{(\alpha\beta\gamma)} W_{3(020)}^{(\alpha\beta\gamma)} \right] - \frac{h_\beta}{2\sqrt{3}} R_{p(010)}^{(\alpha\beta\gamma)} \tag{12}$$

$$S_{p(001)}^{(\alpha\beta\gamma)} = \frac{l_\gamma^2}{4} \left[C_{p5}^{(\alpha\beta\gamma)} W_{1(002)}^{(\alpha\beta\gamma)} + C_{p4}^{(\alpha\beta\gamma)} W_{2(002)}^{(\alpha\beta\gamma)} + C_{p3}^{(\alpha\beta\gamma)} W_{3(002)}^{(\alpha\beta\gamma)} \right] - \frac{l_\gamma}{2\sqrt{3}} R_{p(001)}^{(\alpha\beta\gamma)} \tag{13}$$

where $p = 1,\ldots,6$. The components $R_{p(lmn)}^{(\alpha\beta\gamma)}$ of the vector $\mathbf{R}_{(lmn)}^{(\alpha\beta\gamma)}$ are given by

$$\mathbf{R}_{(lmn)}^{(\alpha\beta\gamma)} = \left[R_{11(lmn)},\ R_{22(lmn)},\ R_{33(lmn)},\ R_{23(lmn)},\ R_{13(lmn)},\ R_{12(lmn)} \right]^{(\alpha\beta\gamma)} \tag{14}$$

These inelastic stress contributions are obtained by integrating the relevant flow rule to yield the inelastic strain at time t.

In conclusion, the integration of the inelastic flow rule at the current time t provides the inelastic strain $\boldsymbol{\varepsilon}^{I(\alpha\beta\gamma)}$ from which the stress terms $\mathbf{R}_{(lmn)}^{(\alpha\beta\gamma)}$ can be determined according to Equation (9). Hence, one can compute the volume-average stress and stress moments $\mathbf{S}_{(lmn)}^{(\alpha\beta\gamma)}$ from Equations (10) to (13). The latter can be used in Equation (63) to obtain the various surface tractions ${}^{(1)}\mathbf{t}^{\pm(\alpha\beta\gamma)}$, ${}^{(2)}\mathbf{t}^{\pm(\alpha\beta\gamma)}$ and ${}^{(3)}\mathbf{t}^{\pm(\alpha\beta\gamma)}$. These can be employed in conjunction with the interfacial and boundary conditions to construct the current system of ordinary differential Equation (79) from which $\mathbf{X}$ at time $t + \Delta t$ can be obtained.

Structural/Acoustic Evaluation of Foam Sandwich Panels

The above two-dimensional wave propagation theory has been applied to model the acoustic attenuation properties of structural panels of the type used in rotary aircraft cabins. These simulations were performed using a "virtual acoustic test chamber", which defines the geometry in which the acoustic properties of the panels are evaluated. The main issue with a simulated test chamber is eliminating the effects of spurious reflections on the "measured" signal. For instance, in Figure 3, the applied cyclic loading, which simulates an acoustic signal, is applied on the lower boundary of the analysis space. The wave travels through the air and then impacts the bottom of the panel. The wave travels through the panel and into the air, where the wave is recorded at a "virtual sensor" location 0.5 cm above the panel surface. The wave then continues through the air to the boundary of the analysis space and is reflected back, eventually making its way back to the top of the panel. Since we are primarily interested in the effects of the panel on the propagating waves without reflected waves from the rear surfaces, we wish to exclude the effects of these latter waves. In order to avoid recording pressures that include the effects of these reflected waves, the dimension of the virtual test chamber behind the panel must be sufficiently long. It was determined that a length of 21 cm was sufficiently long for an applied wave frequency of 10,000 Hz. Note that, as the frequency decreases, this length will increase as a longer time is needed for several waves to pass though the panel to be recorded, but this longer time requirement can allow reflected waves enough time to interfere. It should be noted that noise issues in many rotorcraft cabins tend to occur at frequencies in the range of 1000 to 3000 Hz. Examining these frequencies would require a longer virtual test chamber. Herein, air was assumed to be a fluid possessing no ability to transmit shear stresses whose bulk modulus is given by,

$$K = \rho c_p^{\ 2} \tag{15}$$

where c_p is the velocity of sound in the fluid. The properties employed for air are, $\rho = 0.00129$ g/cm^3 and $c_p = 346$ m/s.

Figure 4 is a plot versus time of an applied 10,000 Hz signal (i.e., pressure wave) and the response at the location of the virtual pressure sensor (0.5 cm above the panel top surface location in the middle of the chamber) in the case of an empty chamber (filled only with air) and in the case of a typical panel. It takes approximately 250 μs for the wave to reach the virtual sensor location. Clearly, a large decrease in the wave amplitude is caused by the presence of the panel.

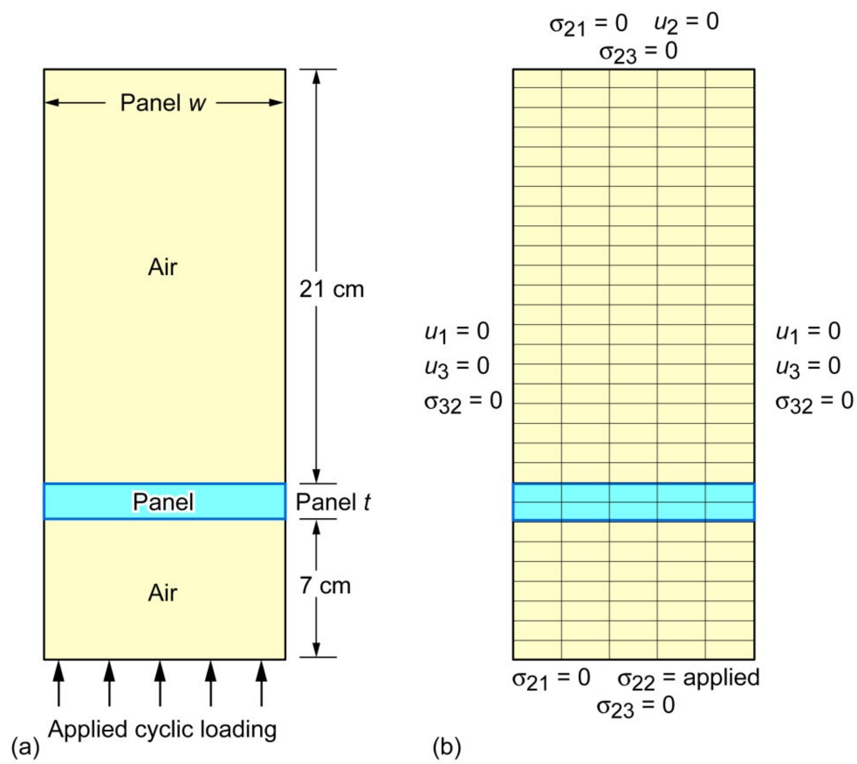

Figure 3.—Virtual acoustic test chamber used to simulate the acoustic behavior of structural panels using the wave propagation theory. (a) Dimensions. (b) Representative discretization and boundary conditions.

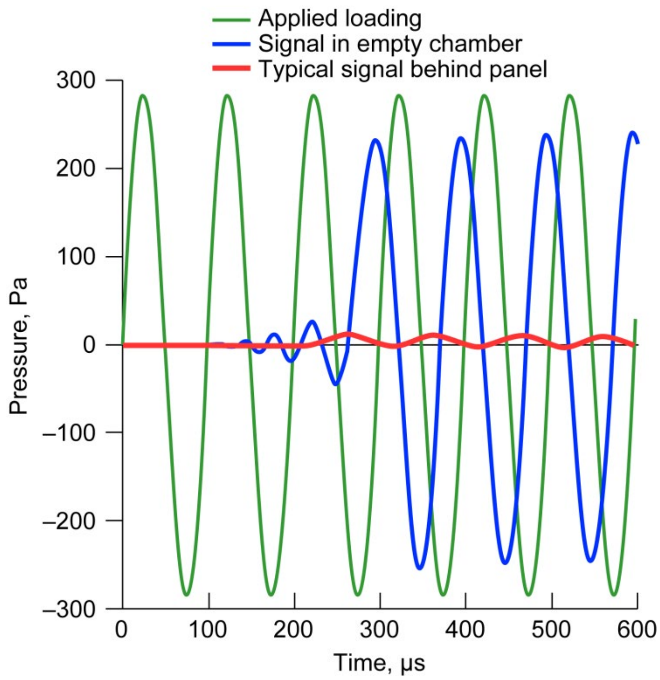

Figure 4.—Example pressure waves recorded at the virtual sensor location 0.5 cm above the panel top surface.

A facesheet thickness study was performed on four different sandwich panels, with Al and IM7/8552 facesheets and two Rohacell foam core densities, using the virtual test chamber (Figure 3). As shown in Figure 5, the total thickness of the panel was kept constant at 2 cm, while the facesheet (FS) thickness was varied between 0.8 and 1.6 mm. The relevant properties of the panel constituent materials are given in Table 1. Note that effective (homogenized) properties are used for the composite facesheet and foam materials, as opposed to modeling individual plies, fiber/matrix constituents, or pores within the foam. Figure 6 is a plot of sound pressure level (SPL) reduction caused by the presence of the panel in the virtual test chamber versus the panel areal mass for each of the four panel types with varying facesheet thickness. Note that, in this figure, the closer given panel design falls to the upper left, the better performance (as high SPL reduction with low mass is desirable).

TABLE 1.—MATERIAL PROPERTIES USED FOR PANEL ACOUSTIC ATTENUATION STUDIES

Property	Aluminum	Quasi-Isotropic IM7/8552	Rohacell 31A Foam	Rohacell 110A Foam
E, GPa	72.4	57	0.036	0.16
ν	0.33	0.32	0.38	0.38
ρ, g/cm^3	2.8	1.578	0.032	0.11

The SPL is given by,

$$\mathrm{SPL} = 20\log_{10}\left(\frac{p_{rms}}{p_{ref}}\right) \tag{16}$$

where p_{ref} = 20 µPa is the standard reference pressure for airborne sound, and the root mean square pressure is given by,

$$p_{\mathrm{rms}} = \sqrt{\frac{1}{t_{av}} \int_0^{t_{av}} [p(t)]^2 \, dt} \quad (17)$$

$p(t)$ is the pressure signal as a function of time, and t_{av} is the duration of the pressure signal.

Figure 6 shows that the denser Rohacell 110 foam core and the aluminum facesheet provide the best overall SPL reduction, but the composite facesheet with the Rohacell 110 provides almost as much SPL reduction at a significantly lower mass. For the Rohacell 110 foam core, increasing the FS thickness does not have much of effect on the SPL reduction. In contrast, the FS thickness has a significant impact on the SPL reduction for the Rohacell 31 core as the contribution of this lower density foam to the panel damping is much lower than in the case of the Rohacell 110 foam core panel. It is noteworthy that the composite facesheet (FS) curves appear as almost an extension of the aluminum FS curves as if the aluminum facesheets continued to become thinner.

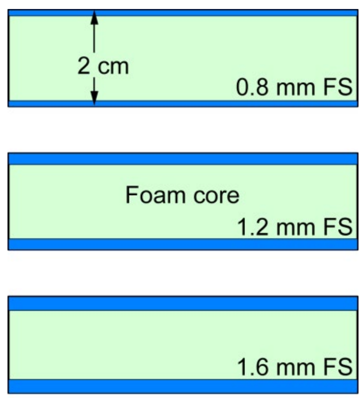

Figure 5.—Foam core panels considered with three different facesheet thicknesses.

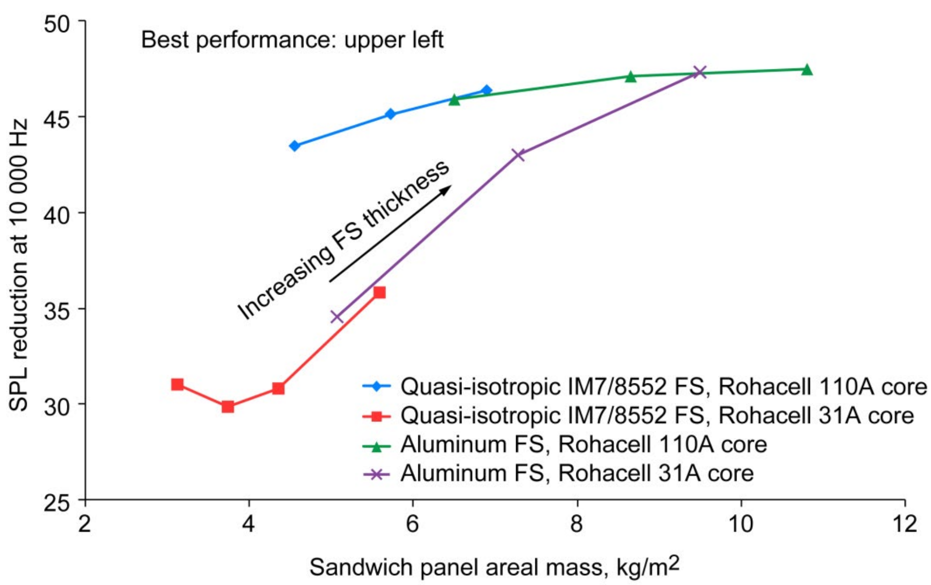

Figure 6.—Areal mass versus SPL reduction for the four panel types simulated.

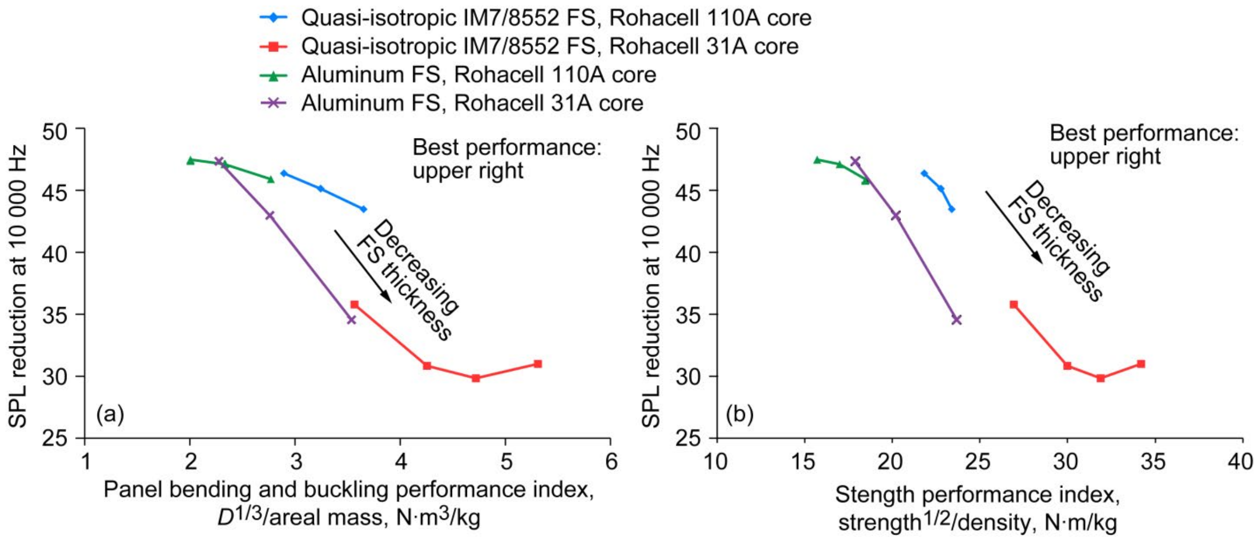

Figure 7.—(a) Panel bending/buckling performance index versus SPL reduction for the four panel types simulated. (b) Panel strength performance index versus SPL reduction for the four panel types simulated.

From Figure 6, it appears that the Rohacell 110 core with thin composite facesheets provides the best overall performance of the panels considered. However, this figure considers only the raw unit mass of the panel and does not account for the panel's structural performance. If instead we plot the SPL reduction versus structural performance indices (Ashby, 2005), as shown in Figure 7(a) and (b), it is clear that the less dense Rohacell 31 core panel with composite facesheets is also quite competitive. The performance indices are associated with the structural efficiency of the panel per unit mass for panel bending and buckling, Figure 7(a), and panel in-plane strength, Figure 7(b). The plots provide a good measure of the trade-off between acoustic performance and structural performance of the panels for lightweight applications. This is particularly important for rotorcraft cabin panels, where interior noise is an important design consideration as is structural mass.

Acoustic Evaluation of Heterogeneous Panels

Here we consider two panels consisting of 75 percent aluminum and 25 percent Rohacell 31A foam, as shown in Figure 8. The first includes two layers of Rohacell foam, while the second has discrete Rohacell 31A inclusions. These panels were simulated in the virtual test chamber shown in Figure 3 at a variety of frequencies. The resulting SPL reductions are plotted versus frequency in Figure 9. Also plotted is the "mass law" for transmission loss through a panel (Fahy, 1985),

$$\mathrm{TL} = 20\log_{10}\left(m_s f\right) - 47 \tag{18}$$

where m_s is the panel areal mass in kg/m^2, f is the frequency in Hz, and TL is the transmission loss (i.e., SPL reduction) in dB. Both panels considered have an identical areal mass of 42.2 kg/m^2; all that is different is the arrangement of the foam and aluminum constituents. Equation (18) provides an engineering estimate of panel SPL reduction in frequencies governed by the mass law, where the material stiffness and microstructure do not play a roll. This is typically in the range of 100 to 1000 Hz, as shown in Figure 10.

Figure 9 shows that the panel with discrete foam inclusions provides more SPL reduction than does the layered panel. This is expected as the discrete inclusions are more effective in converting waves from longitudinal to shear. Both panels considered provide SPL reductions that are lower than the mass law prediction (as expected, see Figure 10). However, at the lower frequencies considered, the predictions associated with both panel types converge and begin to follow the mass law curve. This is because, at lower frequencies, the waves have longer wavelengths and thus interact with the microstructure to a lesser extent. It can also be shown that the results are independent of the stiffness of the panel at these lower frequencies, as predicted by the mass law.

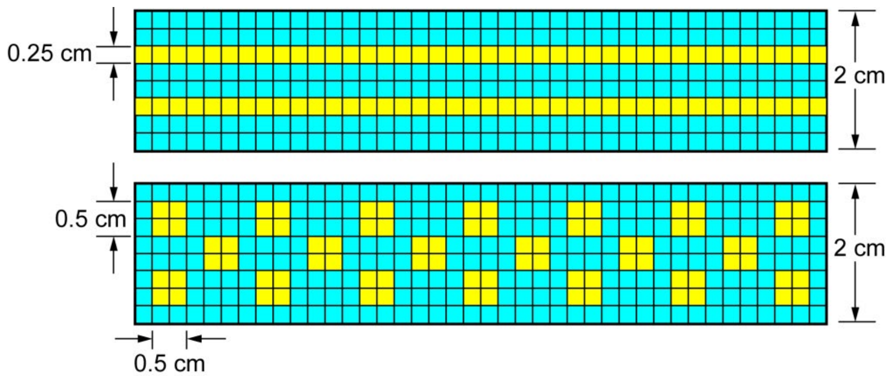

Figure 8.—Heterogeneous Rohacell 31A/aluminum panels considered in the acoustic study.

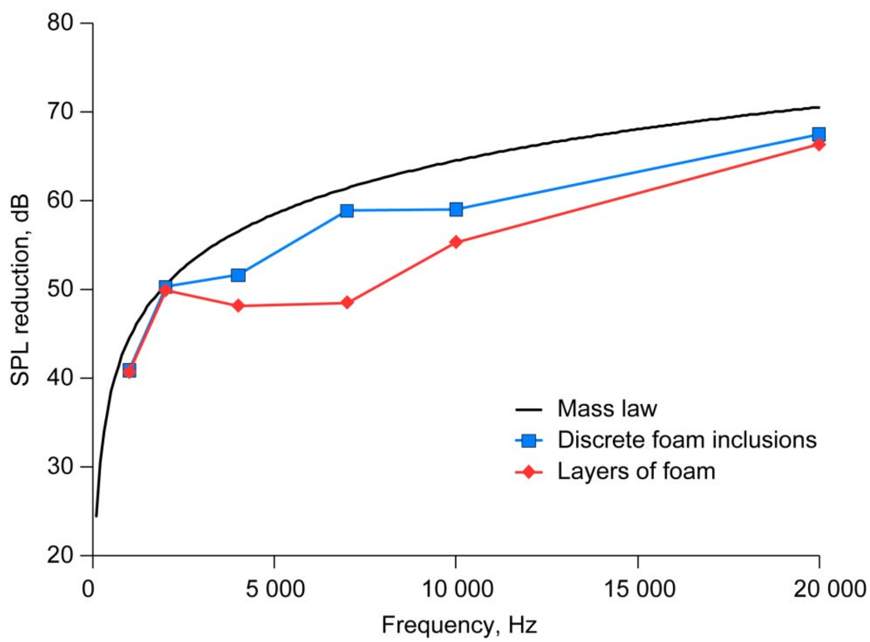

Figure 9.—Heterogeneous Rohacell 31A/aluminum panel SPL reductions at a variety of frequencies.

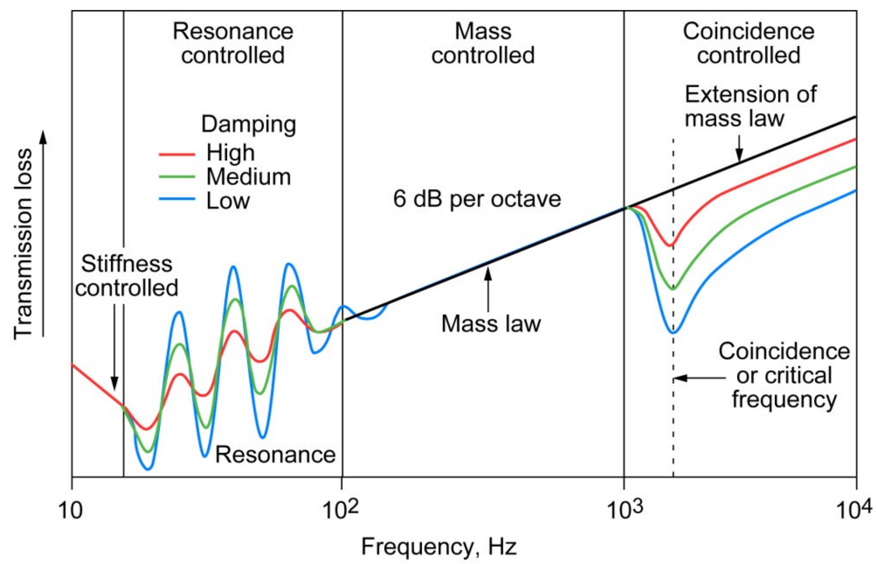

Figure 10.—Typical frequency ranges for the acoustic attenuation properties of structural panels.

Conclusion

An integrated structural/acoustic model has been developed for the analysis of the dynamic response of multiphase panels that are subjected to impulsive loading, such as an acoustic pressure wave. Versions of the model applicable to three-dimensional bodies and two-dimensional bodies were presented. The geometry of the heterogeneous medium is discretized into an arbitrary number of subcells, each of which may contain a distinct solid material, fluid, or a void. By enforcing equilibrium and continuity conditions within and between these subcells, the dynamic response of the medium to time-dependent boundary conditions can be determined. An extension of the model to include inelastic material behavior was also discussed.

The model was applied to analyze the structural/acoustic response of foam core sandwich panels, which are candidates for application in the cabins of rotorcraft. This was accomplished using a virtual test chamber, in which the acoustic wave can be applied to the air surrounding the panel rather than directly to the panel surface. This captures the interaction of the wave with the panel surface rather than assuming a known boundary condition at the panel surface, and is thus more physically representative of the interaction of the structure with the acoustic environment. However, as in real acoustic testing, care must be taken to ensure that reflected waves do not pollute the results so that the true panel acoustic performance is obtained. Various panel designs were compared in terms of their acoustic and structural performance, and it was demonstrated that a trade-off exists between the desire to design panels with high transmission loss (better acoustic performance) and the desire to design panels with the lowest mass (better structural performance).

It is clear that the presented model is capable of evaluating the impact of material and geometric design parameter changes on the structural/acoustic performance of lightweight panels for application in rotorcraft. It’s ease of use and efficiency for performing full dynamic simulations, like those presented herein, make it an attractive alternative to the finite element method for this purpose. Enhancements that would make the model more useful would be an automated ability to alter the applied acoustic wave frequency, while simultaneously adjusting the size of the virtual test chamber to ensure that reflected waves do not influencing the results.

References

Aboudi, J. (1986) Harmonic Waves in Composite Materials, Wave Motion, 8, 289-303.

Aboudi, J. (1987) Transient Waves in Composite Materials, Wave Motion, 9, 141-156.

Aboudi, J. (1988a) Wave Propagation in Damaged Composite Materials, Int. J. Solids and Structures. 24, 117-138.

Aboudi, J. (1988b) Nonlinear Wave Propagation in Laminated Composites, in: Wave Propagation in Structural Composites, ASME AMD-vol. 90, 133-140.

Aboudi, J. and Hevroni, I. (1991) "Wave Propagation in Angle-Ply Laminates" J. Sound Vib., 150, 15-24.

Ashby, M.F. (2005) *Materials Selection in Mechanical Design*, Elsevier Butterworth Heinemann, New York.

Clements, B. E., Johnson, J. N. and Hixon, R. S. (1996), Stress waves in composite materials. Phys. Rev. E, 54, 6876-6888.

Clements, B. E., Johnson J. N. and Addessio, F. L. (1997a), Wave propagation in an epoxy-graphite laminate. J. Appl. Phys. 82, 4831-4837.

Clements, B. E., Johnson, J. N., Addessio, F. L. and Hixon, R. S. (1997b), Impact produced stress waves in composites. J. de Physique IV 7 (Colloque C3), 767-772.

Clements, B. E., Johnson, J. N. and Addessio, F. L. (1998), Wave propagation in laminates: a study of the nonhomogenized dynamic method of cells. Wave Motion 27, 193-209.

Fahy, F. (1985) *Sound and Structural Vibration Radiation, Transmission and Response*, Academic Press, London.

REPORT DOCUMENTATION PAGE	*Form Approved* *OMB No. 0704-0188*

1. REPORT DATE *(DD-MM-YYYY)*
01-10-2012

2. REPORT TYPE
Technical Memorandum

3. DATES COVERED *(From - To)*

4. TITLE AND SUBTITLE
Integrated Structural/Acoustic Modeling of Heterogeneous Panels

5a. CONTRACT NUMBER

5b. GRANT NUMBER

5c. PROGRAM ELEMENT NUMBER

6. AUTHOR(S)
Bednarcyk, Brett, A.; Aboudi, Jacob; Arnold, Steven, M.; Pennline, James, A.

5d. PROJECT NUMBER

5e. TASK NUMBER

5f. WORK UNIT NUMBER
WBS 984754.02.07.03.16.03.02

7. PERFORMING ORGANIZATION NAME(S) AND ADDRESS(ES)
National Aeronautics and Space Administration
John H. Glenn Research Center at Lewis Field
Cleveland, Ohio 44135-3191

8. PERFORMING ORGANIZATION REPORT NUMBER
E-18440

9. SPONSORING/MONITORING AGENCY NAME(S) AND ADDRESS(ES)
National Aeronautics and Space Administration
Washington, DC 20546-0001

10. SPONSORING/MONITOR'S ACRONYM(S)
NASA

11. SPONSORING/MONITORING REPORT NUMBER
NASA/TM-2012-217728

12. DISTRIBUTION/AVAILABILITY STATEMENT
Unclassified-Unlimited
Subject Categories: 39 and 71
Available electronically at http://www.sti.nasa.gov
This publication is available from the NASA Center for AeroSpace Information, 443-757-5802

13. SUPPLEMENTARY NOTES

14. ABSTRACT
A model for the dynamic response of heterogeneous media is presented. A given medium is discretized into a number of subvolumes, each of which may contain an elastic anisotropic material, void, or fluid, and time-dependent boundary conditions are applied to simulate impact or incident pressure waves. The full time-dependent displacement and stress response throughout the medium is then determined via an explicit solution procedure. The model is applied to simulate the coupled structural/acoustic response of foam core sandwich panels as well as aluminum panels with foam inserts. Emphasis is placed on the acoustic absorption performance of the panels versus weight and the effects of the arrangement of the materials and incident wave frequency.

15. SUBJECT TERMS
Wave propagation; Acoustic attenuation; Panels; Foams; Sandwich structures; Sound waves; Dynamic response; Elastodynamics; Transmission loss; Simulation microstructure; Micromechanics

16. SECURITY CLASSIFICATION OF:			17. LIMITATION OF ABSTRACT	18. NUMBER OF PAGES	19a. NAME OF RESPONSIBLE PERSON
a. REPORT	b. ABSTRACT	c. THIS PAGE			STI Help Desk (email:help@sti.nasa.gov)
U	U	U	UU	36	19b. TELEPHONE NUMBER *(include area code)* 443-757-5802

Standard Form 298 (Rev. 8-98)
Prescribed by ANSI Std. Z39-18